

1 **Development of a numerical tool for the seismic vulnerability assessment of vernacular** 2 **architecture**

3 **Abstract**

4 Aiming at protecting the vernacular heritage located in earthquake prone areas, the paper presents the
5 development and validation of the numerical tool that constitutes the core of a novel seismic vulnerability
6 assessment method: Seismic Assessment of the Vulnerability of Vernacular Architecture Structures (SAVVAS).
7 An extensive numerical modeling campaign was carried out to evaluate and quantify the influence of several
8 parameters on the seismic response of vernacular buildings. The results were compiled into a database on which
9 regression analysis could be performed to extract correlations between seismic capacity and qualitative and
10 simple quantitative data that can be obtained from visual inspection.

11 **1. Introduction**

12 Seismic vulnerability assessment methods for the built environment play an important role on risk mitigation
13 because they are the main components of models capable of predicting damage to buildings and estimating
14 losses in future earthquakes. That is why they have become a valuable tool for the preservation of the built
15 heritage, since they allow identifying the most vulnerable elements at risk. As a result, structural retrofiting
16 strategies at an urban or regional level can be defined and optimized by highlighting those buildings where the
17 biggest efforts should be concentrated. This has a particular importance when dealing with the preservation of
18 the built vernacular heritage, which is rarely represented by single structures, but usually involves a group of
19 buildings and settlements within a rural region or within an historical city center.

20 Several definitions and interpretations have been given to vernacular architecture [Rapoport 1972; Rudofsky
21 1990; Oliver 1997; ICOMOS 1999]. A common understanding of this wide concept is that vernacular buildings
22 are usually owner or community built. Thus, they are not designed by specialists but, on the contrary, are part of
23 a process that involves many people over many generations, being based on empirical knowledge and reflecting
24 the tradition and life style of a community, as well as the inhabitant's bonding with the natural environment.
25 That is why vernacular architecture is also often defined as the opposite of high or monumental architecture.

26 Precisely because of its empirical and traditional nature, vernacular architecture is nowadays considered in
27 many places as an obsolete way of building and only valued as part of the region's identity [Correia 2017].
28 Typically, people tend to see vernacular construction technologies as unsafe and eventually abandon and
29 substitute them with modern ones. This leads to a homogenization of the way of building throughout the world,
30 providing a type of architecture that can be observed in any geography, jeopardizing the local building culture.
31 Besides the loss of authenticity, the current global urbanization tendency that results in the adoption of new
32 modern alien technologies enables structures to be erected quickly and cheaply, but not necessarily safely [Degg
33 and Homan 2005]. The risk of vernacular heritage to disappear due to this economic, cultural and architectural
34 homogenization was already highlighted by ICOMOS [1999]. Traditional building knowledge, technologies and
35 materials face subsequently problems of obsolescence in a parallel way [May 2010]. As a result of this
36 progressive abandonment, there is also an increasing vulnerability of vernacular architecture facing natural
37 disasters, including earthquakes.

38 The main objective of the present research is to contribute to the awareness and protection of the vernacular
39 heritage located in earthquake prone areas. For that matter, the present paper proposes the development of a
40 novel seismic vulnerability assessment method particularly adapted for vernacular architecture. There exist a
41 wide variety of methods in the literature suitable for different types of analysis with different goals. The
42 different issues previously discussed introduce some constraints to the development of a seismic vulnerability
43 assessment method adequate to the characteristics of vernacular architecture. First of all, given the typical lack
44 of resources assigned to the study and preservation of the vernacular heritage, the targeted method should be
45 easy-to-use and mostly make use of qualitative data that can be rapidly obtained from simple visual inspections.
46 More detailed and sophisticated approaches that demand a deep investigation of the structures including, for
47 example, historical research, non-destructive evaluation or advanced structural analysis are typically restricted
48 for individual monumental buildings. Secondly, given the great heterogeneity of vernacular architecture in terms
49 of geometry, materials or construction techniques, the new method should also allow the individual assessment
50 of the buildings.

51 The method proposed is referred as Seismic Assessment of the Vulnerability of Vernacular Architecture
52 Structures (SAVVAS). This new method aims at the estimation of the maximum seismic capacity of a building

53 based on the identification and characterization of a set of geometrical, structural, constructive and material
54 characteristics that are more influential in the seismic response of the building. The use of key qualitative and
55 quantitative parameters to evaluate the seismic vulnerability of masonry buildings was firstly proposed by
56 Benedetti and Petrini [Benedetti and Petrini 1984]. They defined a vulnerability index formulation on the basis
57 of a vast set of post-earthquake damage observations and expert judgment. They selected a total of eleven
58 parameters related to four classes of increasing vulnerability and weighted them according to their relative
59 importance in determining the seismic behavior of the building. Each parameter is qualified individually, and
60 the overall vulnerability of the building is calculated as the weighted sum of the parameters, expressed through a
61 vulnerability index (I_V), which can be understood as a measure of the building safety under seismic loads
62 [Barbat et al. 1996]. The vulnerability index method has been extensively applied in Italy [GNDDT 1999] and
63 variations of the method, such as the one proposed by Vicente [Vicente 2008], have been recently implemented
64 in several historic city centers in Portugal [Vicente et al. 2011; Neves et al. 2012; Ferreira et al. 2013].

65 The vulnerability index method and its variations have provided useful and reliable results as a first level
66 approach for large-scale assessments. However, they are based solely on empiric observation and the resulting
67 vulnerability index (I_V) is an empirical factor with no physical meaning. It is usually correlated with an
68 estimated damage for a given earthquake. The present research thus acknowledges the need of strengthening the
69 reliability and robustness of existing methods by gaining a better insight of the seismic behavior of vernacular
70 structures. For this purpose, the SAVVAS method has been developed using advanced numerical analysis. In
71 this work, after the selection of the key parameters, detailed finite element (FE) modeling and nonlinear static
72 (pushover) analysis were used to perform an extensive parametric study. The influence of the selected
73 parameters could thus be evaluated and quantified numerically. The strategy consists of modifying a reference
74 model according to the different parameters considered. The variations on the seismic performance of the
75 structure are analyzed and compared in order to define each parameter influence. The use of pushover analysis
76 allows defining the seismic performance of the building quantitatively, in terms of base shear coefficient. From
77 the extensive numerical analysis, classes of increasing seismic vulnerability could be also established for each
78 parameter.

79 The results of the extensive numerical parametric campaign could be assembled into a database. A statistical
80 approach was thus followed for the development of the SAVVAS method, based on quantitative data analysis
81 and Knowledge Discovery in Databases (KDD), using Data Mining (DM) techniques. These techniques allowed
82 obtaining regression models that intend to predict the seismic capacity of vernacular structure using as inputs
83 simple variables based on the selected key vulnerability parameters. These regression models are the main
84 component of the SAVVAS method.

85 The use of an analytical process instead of an empirical one to develop an expedited method for the seismic
86 vulnerability assessment of vernacular structures is considered a step forward in the contribution to scientific
87 knowledge. The first part of the present paper shows in detail the process followed to obtain the regression
88 models of the SAVVAS method. Secondly, the paper presents the validation of these regression models using
89 numerical and experimental works gathered from the literature that deal with the seismic analysis of traditional
90 masonry constructions. The regression models are applied to a total of six cases collected and the predictions are
91 compared with the results provided by the literature. After the validation of the prediction capability of the
92 regression models, the SAVVAS formulation is presented at the end of the paper as the main outcome, together
93 with a summary of the steps that need to be followed to apply it.

94 **2. Numerical parametric study for the definition of seismic vulnerability classes**

95 The idea behind the SAVVAS method consists of developing a novel seismic vulnerability assessment method
96 that is able to estimate the seismic capacity of vernacular buildings in quantitative terms. The quantification of
97 the seismic capacity required an extensive numerical parametric study, designed according to the parameters
98 considered to be more influential in determining the seismic behavior of vernacular buildings. This study helps
99 understanding the seismic behavior and resisting mechanisms of vernacular constructions that present different
100 characteristics in terms of construction, geometry and materials.

101 The numerical analysis is based on FE modeling and pushover analysis. FE modeling following a common
102 macro-model approach has already been extensively and successfully applied with the aim of analyzing the
103 seismic behavior of complex masonry and rammed earth structures [Mallardo et al. 2008; Lourenço et al. 2011;
104 Saloustros et al. 2014; Karanikoloudis and Lourenço 2018]. Pushover analyses with distribution of forces

105 proportional to the mass is also a generally accepted and recommended tool used for the seismic assessment of
106 existing masonry buildings without box-behavior [Lourenço et al. 2011]. This approach allows determining the
107 ability of the building to resist the characteristic horizontal loading caused by the seismic actions taking into
108 account the material nonlinear behavior. Despite the limitations of simulating the earthquake loading as a set of
109 equivalent static forces, pushover analysis is a powerful tool since it can be performed with relatively low
110 computational efforts in comparison with other more sophisticated nonlinear analysis, such as nonlinear
111 dynamic time-history analysis.

112 The development of the new method firstly required to identify and define a number of parameters that
113 represent appropriately distinctive characteristics of vernacular buildings and influence their seismic behavior.
114 The definition of these seismic vulnerability assessment parameters was based on the work developed by other
115 authors that have proposed different vulnerability index formulations [Benedetti and Petrini 1984; Sepe et al.
116 2008; Boukri and Bensaibi 2008; Vicente 2008; Ferreira et al. 2014; Shakya 2014] and on the earthquake
117 performance of vernacular constructions reported in past earthquakes [Blondet et al. 2011; Bothara et al. 2012;
118 Neves et al. 2012; Sorrentino et al. 2013; Gautam et al. 2016]. It should be noted that the SAVVAS method has
119 been developed with a main focus on vernacular architecture typologies whose structural system typically
120 consists on load bearing masonry or earthen walls as the main vertical resisting elements, coupled with
121 horizontal timber diaphragms. Parameters are selected according to the singular behavior of these structural
122 types, acknowledging that many vernacular constructions around the world share a similar concept at the
123 structural level. The ten parameters finally selected are shown schematically in Figure 1.

124 The definition of classes of increasing seismic vulnerability for each parameter is also based on the approach
125 proposed by existing vulnerability index methods [Benedetti and Petrini 1984]. The methodology adopted for
126 the definition of the seismic vulnerability classes consists of seven clearly defined steps that are presented in
127 Figure 2, using one of the parameters as an example. The readers are referred to Ortega [Ortega 2018] for a full
128 detailed explanation of the parametric study performed and the resulting seismic vulnerability assessment
129 classification obtained for each parameter.

130 The first step involves the preparation of reference FE models based on typical vernacular stone masonry and
131 rammed earth constructions targeted by the SAVVAS method (Figure 3). These reference models are prepared

132 in a generic way so that they can easily accommodate the variations required to assess the influence of the
133 different parameters. Several reference models are constructed for the evaluation of each parameter, aiming at
134 providing a more comprehensive understanding of each parameter influence on buildings showing different
135 characteristics. As an example, Figure 2 shows the two reference models prepared for the parametric analysis
136 aimed at defining the seismic vulnerability classes of P2 (maximum wall span): (1) one-floor rammed earth
137 building with flexible diaphragm; and (2) two-floor rammed earth building with rigid diaphragm. The use of
138 these two different building typologies as reference models allows understanding the influence of the maximum
139 wall span when the building is prone to show an out-of-plane failure mode and when the building is prone to
140 present in-plane collapse mechanisms. After the definition of the different reference models, the second step
141 consists of preparing sets of models by modifying each reference model according to a range of variation
142 established for each parameter, taking into account typical values observed within vernacular architecture.

143 Once all the models from each set are constructed, they are subjected to a pushover analysis in the direction in
144 which the parameter under evaluation is supposed to have a greater influence. Continuing with the example
145 above, parameter P2 evaluates the variations in the response of the building when the maximum length of a wall
146 prone to out-of-plane movements varies. Thus, the direction selected for the pushover analysis had to be
147 perpendicular to the walls whose span is being modified. All models from each set of models are then tested in
148 the same direction. DIANA software [TNO 2011] was used for the construction of the models and to perform
149 the pushover analyses. There are some modeling specifications that are shared by all the models constructed for
150 the parametric analysis. Walls are simulated with ten-node isoparametric 3D solid tetrahedron elements
151 (CTE30), using at least two elements within the thickness. When modeled, floors are assumed to be composed
152 by: (a) timber beams simulated using three-node beam elements (CL18B); and (b) cross-board sheathing,
153 modeled using six-node triangular shell elements (CT30S). The roof is modelled as distributed vertical load
154 along the load bearing walls and, when expected to exert thrust to the walls, a distributed horizontal load is also
155 applied at the top of the walls. The displacements of the walls elements at the base are fully restrained.

156 Different materials are considered for the walls (“parameter P3”), from earthen materials (namely adobe
157 masonry or rammed earth) to brick and stone masonry of different quality. Timber is used for the lintels and
158 floor construction elements. Only the materials used for the walls are considered to present nonlinear behavior

159 and the material model adopted is a standard isotropic Total Strain Rotating Crack Model (TSRCM). This
160 model describes the tensile and compressive behavior of the material with one stress-strain relationship and
161 assumes that the crack direction rotates with the principal strain axes. The tension softening function selected is
162 exponential and the compressive function selected to model the crushing behavior is parabolic. It was selected
163 because of its robustness and simplicity, showing successful results in previous analysis of complex stone
164 masonry and earthen structures [Miccoli et al. 2014; Lourenço et al. 2015; Karanikoloudis and Lourenço 2018].
165 Timber elements were always considered to present elastic behavior. The material properties adopted varied for
166 the different models constructed for the parametric analysis and are based on data collected from different
167 authors and codes [NTC 2008; Lourenço 2009; Gomes et al. 2011; Angulo-Ibáñez 2012; Gallego and Arto
168 2014]. Other model details vary among the different models, such as the geometry and the level of connection
169 between the structural elements, see [Ortega 2018] for full details.

170 The fourth and fifth steps are intended to analyze the results of the pushover analyses carried out on each model
171 from each set to obtain a better understanding of the seismic behavior of vernacular buildings. Step four aims at
172 understanding how the seismic response of the building changes in terms of damage patterns and failure
173 mechanisms according to the variations in the parameter under evaluation. Step five analyzes the variations in
174 the seismic behavior of the building in terms of the pushover curve. Pushover analyses allow describing the
175 global seismic response of the structure and the formation of global collapse mechanisms in terms of the
176 capacity or pushover curve. This curve is given as a relation between the base shear coefficient or load factor
177 (i.e. the ratio between the horizontal forces at the base and the self-weight of the structure, expressed as an
178 acceleration in terms of g) and the displacement at the control node (usually taken as the node where the highest
179 displacements take place). It is noted that this node may vary according to the collapse mechanism obtained,
180 which can differ between buildings. Thus, the curves are representative of the global structural behavior of the
181 different buildings subjected to horizontal loading, not individual structural elements composing the buildings.

182 Furthermore, in order to have a common basis of comparison of the seismic capacity of the buildings in
183 quantitative terms, four structural limit states (LS) associated to specific damage levels exhibited by the
184 structure were defined following recommendations available in the literature [Rota et al. 2010; Mouyiannou et
185 al. 2014]. The LS are determined according to the pushover curve obtained for each building (Figure 4). LS1 is

186 associated to the Immediate Occupancy Limit State before which the structural behavior of the building is
187 essentially elastic, and it can be considered as fully operational. LS1 thus corresponds to the onset of cracking,
188 which is assumed to start after a reduction of the initial stiffness of the global response of the building up to 2%.
189 It is noted that the value is relatively low but is related to the low tensile strength of the materials considered in
190 this study and is defined after observing that the first cracks in the numerical models are visible after this
191 reduction of the initial stiffness. LS2 is associated to a Damage Limitation Limit State. It depicts the transition
192 between a state where the structure is still functional, showing minor structural damage and cracks, and a state
193 of significant damage. The definition of LS2 from the pushover curve is made by satisfying two energy criteria:
194 (1) the first energy criterion assumes that the area below the three-linear curve formed by LS1, LS2 and LS3
195 coincides with the area below the pushover curve from LS1 to LS3; and (2) the second criterion assumes that
196 the LS2 point is on the slope associated to the secant stiffness corresponding to 70% of the maximum strength.
197 LS3 is defined by the load factor corresponding to the attainment of the building maximum strength. It is
198 referred as Life Safety Limit State. Finally, LS4 refers to the Near Collapse Limit State and corresponds to the
199 point where the building resistance deteriorates below an acceptable limit, which is set at the 80% of the
200 maximum strength, following recommendations by Eurocode 8 [EN 1998-3 2005].

201 Step five thus consists of transforming the pushover curves of the buildings into four-linear capacity curves
202 according to the points associated to each LS. Through these capacity curves, the seismic behavior of each
203 building is described by four equivalent static horizontal loads (load factors) that the buildings can withstand
204 before reaching each LS. However, they also provide information about the deformation capacity of the
205 building, allowing an easier and quantitative comparison between the structural response of the models from
206 each set in terms of capacity, stiffness and ductility.

207 The sixth step consists of comparing the values of load factor corresponding to LS1 and LS3 for the different
208 models within each set. LS2 and LS4 are not included because they are mathematically determined through LS1
209 and LS3. The load factor variations for LS1 and LS3 can be expressed in terms of a percentage normalized
210 using the maximum value of load factor obtained among the buildings analyzed within the set. This procedure
211 results in the construction of curves that show in a clear manner the variation of the seismic capacity of the
212 building as a function of the variations defined for each parameter (Figure 2).

213 Finally, the seventh and last step consists of the definition of the seismic vulnerability classes according to the
214 variation of the load factor corresponding to the attainment of the maximum capacity of the building (LS3). The
215 criterion followed for the definition of the typical four vulnerability classes of increasing vulnerability consists
216 of dividing equally the total range of variation within each set into four parts. Each interval is associated with a
217 vulnerability class and buildings are classified according to the interval they lie within, see Figure 2. It is noted
218 that the ranges of variation obtained for each set can differ, resulting in differences in the definition of the
219 seismic vulnerability classes. The final classification is made by adopting the most unfavorable class.

220 **3. Methodology adopted to obtain the regression models of the SAVVAS method**

221 In total, the parametric study carried out involved the construction of 277 numerical models with varying
222 geometrical, construction, material and structural characteristics. Since most models were analyzed in the two
223 orthogonal directions, results from more than 400 pushover analyses were obtained. This allowed determining
224 the global seismic response of each building in different seismic loading directions. The results of each
225 pushover analysis performed on each numerical model could compose a wide, reasonably robust, database
226 containing two main pieces of information: (1) the differing characteristic of the numerical models according to
227 the ten key parameters selected; and (2) the seismic load capacity of the different buildings, defined in terms of
228 load factors leading to the attainment of four damage limit states (LS1, LS2, LS3 and LS4).

229 The application of DM algorithms to extract models or patterns that explain relationships between variables
230 from databases is one of the main steps of KDD [Fayyad et al. 1996]. The employment of these tools allows
231 analyzing the complex database obtained from the numerical analyses performed, which presents a large
232 number of variables and complex and unclear relationships among them. The SAVVAS method arises precisely
233 from the intention of delving more deeply into the research question of whether the simple key parameters
234 variables selected can be used to predict the seismic load capacity of vernacular buildings. The final objective of
235 the method is to derive regression models able to quantitatively estimate a value of a load factor that causes the
236 structure to reach the different LS, which can later be correlated with different degrees of structural damage
237 suffered by the building. Moreover, since the load factors that define each LS are expressed in terms of g , they
238 can be compared in a straightforward way with an expected seismic event. The seismic input used for

239 comparison is expressed in terms of Peak Ground Acceleration (PGA) or, when a more refined assessment is
240 required, the site response spectra and the building fundamental period can be used to take into account specific
241 accelerations adapted to each building and site.

242 There are several DM algorithms that can be applied for the desired deeper analysis and the extraction of
243 patterns explaining relationships between variables, such as multiple linear regression, artificial neural networks
244 (ANN), support vector machines (SVM) and decision trees. There is an increasing amount of research in
245 different fields that make use of the abovementioned techniques. This includes research in structural engineering
246 where, for example, DM techniques have been widely applied to formulate models able to predict the
247 mechanical properties of different materials based on experimental data [Baykasoglu et al. 2008; Miranda et al.
248 2011; Garzón-Roca et al. 2013a Martins et al. 2014; Martins et al. 2018] or the structural behavior of different
249 structural elements [Marques and Lourenço 2013; Garzón-Roca et al. 2013b; Plevris and Asteris 2014; Aguilar
250 et al. 2016]. This exemplifies that there is an increasing research focus on developing regression models for the
251 prediction of the mechanical properties of different materials and the structural behavior of different structural
252 elements. However, with the exception of [Garzón-Roca et al. 2013b], who used as the database for developing
253 the ANN models the results of a parametric study with finite elements comprising 3700 models [Sandoval and
254 Roca 2012], all abovementioned studies have developed the models based on large databases of experimental
255 data. This research work makes use of a database composed solely of numerical data obtained from the results
256 of the nonlinear parametric study carried out.

257 **3.1. Methodology**

258 Figure 5 presents an overview of the steps of the methodology adopted to obtain the regression models
259 necessary for the development of the SAVVAS method. The first step concerns the organization of the database.
260 The target data include the load factor corresponding to the attainment of LS1, LS2 and LS3. The load factor
261 defining LS4 is not taken into consideration because it is by definition proportional to the load factor defining
262 LS3. These three load factors associated to the different LS are considered to define the seismic response of the
263 buildings because they depict the seismic load (in terms of g) that would cause the building to reach different

264 damage levels. The regression models are thus intended to predict these three LS using as the input simple
265 variables based on the previously selected parameters.

266 Since the SAVVAS method relies directly upon the regression models, an effort was placed on increasing their
267 prediction accuracy. Thus, while some of the parameters can be defined by the seismic vulnerability classes
268 previously defined, others could be more precisely described using more specific quantitative attributes. For
269 example, P2 (maximum wall span) can be directly defined by the span (in m), instead of by the vulnerability
270 class. The same occurs for P1, defined by the wall slenderness ratio (λ), P8, defined by the number of floors (N)
271 of the building and P10, defined by the in-plane index (γ_i). It should be noted that the in-plane index is defined
272 as the ratio between the in-plane area of earthquake resistant walls in each main direction (A_{wi}) and the total in-
273 plane area of the earthquake resistant walls (A_w), see Figure 1. In the particular case of P7, which concerns the
274 amount and area of walls openings, the parameter was also further divided into two parameters, aiming at
275 distinguishing between the area of wall openings at the walls perpendicular to the loading direction (P7a) from
276 the area of wall openings at the walls parallel to the loading direction (P7b). The remaining parameters,
277 including the type of material (P3), the quality of the wall-to-wall connections (P4), the horizontal diaphragms
278 (P5), the roof thrust (P6) and the previous structural damage (P9), are defined as a function of their class, in
279 qualitative terms. Thus, they are described in a discrete form, assuming four countable numbers from 1 to 4,
280 associated to the classes A to D, respectively.

281 As a result, the data was structured in a database composed of 14 attributes: (a) eleven variables associated to
282 the parameters; and (b) three variables with the values of load factor associated to LS1, LS2 and LS3 obtained
283 for each model. The parameters variables are either: (1) expressed in a discrete form from 1 to 4 when the
284 parameters are described by classes; or (2) expressed as continuous variables using different units depending on
285 the parameter. The load factors are all continuous variables expressed in g , typically ranging from 0 to 1.

286 In terms of applied DM algorithms, the SAVVAS method explores the use of two different techniques to
287 develop the regression models: (a) multiple linear regression (MR); and (b) artificial neural networks (ANN).
288 Nevertheless, it is noted that the ANN models are mainly developed for reference and comparison purposes,
289 intended to show a research path open to further research. The focus is here placed on multiple regression
290 models, whose physical meaning is easier to interpret [Miranda et al. 2011]. The resulting regression models

291 obtained are able to predict the seismic behavior of vernacular buildings based on the simple eleven parameters
292 variables defined. They constitute the core of the SAVVAS method.

293 **3.2. SAVVAS database**

294 A preliminary data analysis performed in a first stage concluded that the extension of the database was not
295 deemed enough to define robust regression models. Therefore, additional numerical models were built in order
296 to enlarge the database, intending to have a more balanced distribution of buildings belonging to the different
297 classes for each parameter. The database needed to be diverse and representative enough of all classes of each
298 parameter. Considering the pattern of variability within each parameter variable (i.e. the distribution of
299 buildings belonging to each class), a lack of balance (or asymmetry) was detected. Due to the use of reference
300 models showing similar initial conditions for the definition of the classes, some seismic vulnerability classes in
301 certain parameters are more frequent than others. The first step of the database extension process consisted of
302 identifying those classes in each of the ten parameters that were less represented in the original database. The
303 main criterion applied for the enlargement of the database was to ensure that there are a minimum of 25 models
304 representing each parameter class, in order to contain a meaningful statistical amount for all of them.
305 Additionally, some new models were constructed aimed at assessing the efficiency of traditional earthquake
306 resistant techniques for vernacular architecture [Ortega et al. 2018]. The results of these analyses were also
307 added to the initially constructed database. In total, the extension process led to a final database composed of
308 567 results obtained from pushover analyses performed on FE models. The precise information on the process
309 of extension of the database is detailed in [Ortega 2018].

310 Several operations can be also applied on the attributes selected for the database in order to eventually help
311 improving the prediction capabilities of the regression models. For instance, the dependence of the output
312 variable on a specific predictor may be not linear, which can lead to errors in the prediction. Different
313 transformations of the input and output data, such as logarithms and powers, were considered to help to linearize
314 this relationship and to better describe the effect of each parameter in the seismic behavior of the building.
315 Indeed, all the output variables had to be transformed in order to assure that the predicted values from the
316 multiple linear regression models are always positive. The output variables are the load factors that measure the

317 seismic action that causes the building to reach specific LS and they are expressed in terms of g . Therefore, as a
318 measure of the seismic load, they cannot be negative. However, in some specific cases, the load factor defining
319 LS1 can be 0, if the building is assumed to present an initial level of structural damage (e.g. because of the state
320 of conservation or the roof thrust), but can never show values below 0. This led to the adoption of a logarithmic
321 transformation of the three output variables (LS1, LS2 and LS3), since the predicted values from a log-
322 transformed regression will never be negative, respecting the physical meaning of the variable. The logarithmic
323 transformation involves the adoption of a natural logarithm of the output variables. It should be noted that, since
324 there are zero values among the data of the variable LS1 and there is no logarithm of the value zero, a constant
325 ($c = 0.01$) was added to all LS1 values before applying the log transformation. A small positive constant
326 between 0 and the smallest non-zero observation that preserves the order of magnitudes of the data is usually
327 recommended [McCune and Grace 2002; Field et al. 2012].

328 As a summary, the list of the input and output transformed and untransformed variables considered, together
329 with general statistical measurements, is presented in Table 1. It should be noted that the transformations of the
330 variables result from a trial and error process and only those that revealed to have a notable influence in
331 improving the prediction capabilities of the regression models are presented.

332 **4. Regression models**

333 The statistical analysis and the definition of the regression models are carried out by using R open source
334 software [R Development Core Team 2008]. Different regression models were prepared and compared in order
335 to conclude with the final formulation of the SAVVAS method. The discussion of the results presented herein
336 also allowed a deeper understanding of the relationships among the parameters and their influence on the
337 seismic behavior of vernacular buildings. The selection of the final expressions is based on a compromise
338 between the accuracy in the prediction and the choice of patterns whose physical meaning is more
339 understandable.

340 **4.1. Multiple linear regression models**

341 The first DM technique applied is multiple linear regression (MR). Regression analysis is a popular statistical
342 method used to study the relationship among variables [Kottegodo and Rosso 2008]. In the present case, MR is
343 intended to investigate the dependence of LS1, LS2 and LS3 (output variables) on the eleven key parameter
344 variables (the input variables), as well as to define and quantify the relationship among them through a
345 mathematical model. A multiple regression model is required because there is more than one input variable
346 [Montgomery et al. 2012]. The relationship between variables is often very complex and the simplest approach
347 consists of fitting a multilinear equation to the data:

$$Y = \beta_0 + \beta_1x_1 + \beta_2x_2 + \dots + \beta_kx_k + \varepsilon \quad (1)$$

348 where Y is the output variable and k is the number of input explanatory variables (x_k). The parameters β_k are
349 called the regression coefficients and ε is the error. The line defined by the regression equation (1) describes
350 how the response changes according to the explanatory variables. Different regression models were prepared
351 using always multiple regression analysis, but varying the input variables taken into consideration. This section
352 is thus meant to provide a comparison of the performance of the different models concerning their capability in
353 predicting the load factors associated to the different limit states (LS). In total, six regression models are
354 presented and discussed next.

355 The first regression model (*MRO*) is a simple model that uses as input only the seismic vulnerability classes for
356 all ten parameters (i.e. discrete values between 1 and 4) and is mainly meant to serve as reference. Then, aiming
357 at further improving the precision of the regression models, five more regression models were constructed
358 assuming different combinations of: (a) input variables; (b) transformations of the attributes; and (c) interactions
359 among the attributes. It is noted that, in a first step, the regression models are constructed using LS3 as the
360 output variable. Different combinations were thus created using the continuous variables and transformations
361 defined and presented in Table 1 and the interactions among them. This latter condition was considered as a
362 very critical aspect because the results of the numerical parametric study confirmed that the influence of some
363 parameters is sensitive to the variations of other parameters. Thus, several interactions between the parameters

364 were tested in different regression models. For example, when the building presented a rigid diaphragm able to
365 distribute the load among all structural elements ($P5$), the influence of the area of wall openings in the in-plane
366 walls ($P7b$) is decisive. On the contrary, if the buildings present a flexible diaphragm, the failure of the building
367 is typically controlled by the out-of-plane failure of the walls and, thus, the area of wall openings in the in-plane
368 walls has a negligible effect on the response of the building. That is why the interaction between parameters that
369 influence themselves mutually was introduced in the multiple regression models. Considering the previous
370 example, a new interaction term composed by the product $P5 \times P7b$ can be included in the regression models,
371 keeping also the independent terms $P5$ and $P7b$. With the new predictor term, the influence of $P7b$ on the
372 variation of $LS3$ is different for different values of $P5$, reflecting better what was observed in the numerical
373 parametric study.

374 The six different regression models with different sets of input variables and considering the different
375 interactions among them are shown in Table 2. Regarding the notation adopted, it is noted that label I (ex.
376 MR_{II}) is added to the models that include interaction among parameters. The table shows measurements of the
377 predictive performance of the models in terms of error and coefficient of determination (R^2). It should be noted
378 that the k -fold cross-validation method, with $k = 10$, was applied for developing the models and assessing the
379 predictive capacity of the models, since it is considered as one of the most robust methods [Cortez 2010]. The
380 method consists of randomly partitioning the data into k sets of roughly the same size. A model is then trained
381 using all the sets except the first subset, which is used for testing, calculating the prediction error and accuracy
382 of the model. The same operation is repeated ten times (for each partition) and the performance of the model is
383 evaluated by averaging the errors (MAE and RMSE) of the different test sets. Finally, once the most appropriate
384 set of input variables and intersections is selected, the final models are developed using all the data.

385 The models show different levels of complexity in order to find the abovementioned compromise between
386 accuracy in the prediction and a clear and simple physical meaning. The adoption of more accurate attributes to
387 define the parameter variables in MRI , together with the logarithmic transformation of the output variable,
388 already results in a significant improvement in its prediction performance in comparison with the MRO model.
389 However, the models that consider interaction among parameter showed an overall improvement with respect to
390 two models MRO and MRI , reaching values of R^2 close to 0.9. The introduction of the interactions leads to an

391 improvement in the prediction capability, reducing the errors, but the level of complexity of the formulation
392 increases as well. This is the case of models *MR_I1*, *MR_I2* and *MR_I3*. The use of a robust cross-validation
393 method reduces the risk of overfitting, i.e. the risk of creating excessively complex models that fit very well the
394 data because of describing random error instead of the actual patterns of variability. However, the limitations of
395 the database, such as the narrow range of variability within some parameters, may result in models that are very
396 adequate for this dataset but are not so representative of scenarios outside of it. That is why, in the end, a more
397 general expression was preferred. *MR_I4* tried to simplify the model to the maximum extent possible in terms of
398 number of predictors, using only those showing the highest relative importance in the prediction. It shows a
399 good performance, but it neglects some parameters that proved to be also influential in the parametric analyses
400 and thus can be critical as well when evaluating other sets of data. Figure 6 shows the predicted versus observed
401 values obtained for the six models with different sets of input variables and interactions.

402 After evaluating the performance of the different models, as well as the compromise between simplicity and
403 prediction capability, model *MR_I1* was adopted as MR_LS3 due to its relatively simple formulation. It uses all
404 the untransformed input variables for the prediction, but adds the interaction between P5 and P7b that had an
405 obvious influence and proves to have an important prediction weight. By adding this interaction term, the
406 regression model reaches a R^2 of 0.877, explaining 88% of the variation of the output data, which is considered
407 satisfactory. It should be highlighted that it provides a quite accurate value of LS3 based only on the ten
408 parameter variables and on one single simple interaction. The errors are also reduced with respect to models
409 *MRO* and *MRI*, showing a maximum error of 0.318g. The predicted versus observed values obtained for this
410 model are further shown in Figure 7a. Figure 7b presents the predicted value with the residuals. The graph
411 shows clearly that the highest deviations occur for higher values of LS3, approximately over 0.6g. Those
412 buildings with $LS3 > 0.6g$ can be already considered to have low vulnerability so that the accuracy of the model
413 is less critical. The main part of the dataset includes models with values of LS3 ranging from 0.15g to 0.6g and
414 is well matched. Besides, all values bounce over the 0 line, but the great majority of them lies between -0.1g and
415 0.1g. Only 16% of the models are outside this range, i.e. showed an absolute error higher than 0.1g. Thus,
416 results were deemed acceptable to adopt *MR_I1* as the regression model for LS3. By comparing the models
417 shown in Figure 6, it is clear that, with the exception of the simple *MRO* regression model, the performance of

418 the different models is similar in terms of accuracy of the prediction, which justifies the selection of *MR_II* as
 419 the final regression model, given its simpler formulation. The regression equation obtained from *MR_LS3* is:

$$\ln(LS3) = 2.523 - 0.044 \times \lambda - 0.063 \times s - 0.238 \times P3 - 0.186 \times P4 - 0.279 \times P5 - 0.091 \times P6 + 0.273 \times P7a - 2.833 \times P7b - 0.396 \times N - 0.156 \times P9 + 0.684 \times \gamma_i + 0.438 \times P5 \times P7b \quad (2)$$

420 The regression models intended to predict the load factors corresponding to LS1 and LS2 were constructed
 421 following the same procedure previously explained for LS3. Only the final models adopted are presented and
 422 discussed. Figure 8 presents the predicted versus observed values of both models. Table 3 shows the variables
 423 used for the final models constructed and the measurements of the performance, in terms of errors (MAE and
 424 RMSE) and coefficient of determination (R^2).

425 In the case of the regression model prepared for the prediction of the load factor associated to LS1 (*MR_LS1*),
 426 different sets of input variables and different interactions were trained and tested until reaching the final
 427 formulation. As an example, particular attention was put in the use of the variables representing the seismic
 428 vulnerability parameters P6 (roof thrust) and P9 (previous structural damage), which can lead LS1 to take zero
 429 values for some classes. The logarithmic transformation of both variables allowed capturing properly this
 430 characteristic. The same parameters interaction used for the selected *MR_II* model for LS3 was also adopted for
 431 this model ($P5 \times P7b$). The overall behavior of the model is considered quite acceptable for the relatively
 432 simple formulation obtained (Figure 8a), presenting low errors and a high R^2 of 0.811. The final regression
 433 equation from *MR_LS1* model reads:

$$\ln(LS1 + c) = 2.201 - 0.061 \times \lambda - 0.099 \times s - 0.712 \times \ln(P3) - 0.156 \times P4 - 0.289 \times P5 - 0.521 \times \ln(P6) - 3.668 \times P7b - 0.847 \times \ln(N) - 2.31 \times \ln(P9) + 0.679 \times P5 \times P7b \quad (3)$$

434 In the case of the regression model constructed for the prediction of the load factor associated to LS2, instead of
 435 using the parameter variables, the variables previously used as output (LS1 and LS3, expressed in g) are now
 436 used as the only input for the model. These new inputs are selected because the definition of this damage limit
 437 state is mathematically dependent on LS1 and LS3 [Ortega 2018]. Therefore, it can be calculated using solely
 438 those two input variables. This simplified its calculation while leading to very accurate predictions and an
 439 almost perfect correlation with much reduced errors (Figure 8b). The final regression equation from *MR_LS2*
 440 model is:

$$LS2 = 0.152 \times LS1 + 0.781 \times LS3 \quad (4)$$

441 **4.2. Artificial neural networks**

442 An artificial neural network is a computational scheme whose basic unit are neurons organized in layers. Each
443 neuron receives a series of inputs, multiplies them by previously defined weights and combines them adding a
444 predetermined constant called bias to send an output. Most common neural networks are composed by different
445 parallel layers of neurons. The first layer contains the input variables, the intermediate layer or layers are known
446 as hidden layers, and the last layer contains the output. Typically, besides the predefined input and output
447 variables that are intended to be predicted, an ANN is also described by the number of hidden layers and the
448 number of neurons in each hidden layer. This work uses a feedforward network, which means that the
449 connections always go from inputs to outputs (there is no connection between the neurons within the same
450 layer) and there are no cycles in the network. It uses the sigmoid function as the activation function, which is a
451 particular case of logistic function that is commonly used within ANN architecture [Montgomery et al. 2012;
452 Günther and Fritsch 2010]. Finally, the learning process algorithm applied is back propagation, which consists
453 of setting initial random values for the weights and biases, leading to a specific output. The error is measured
454 and propagated backwards in order to adjust the weights and biases. This process is repeated so that gradually
455 the actual output from the model gets closer to the desired output after rounds of testing, until reaching a
456 minimum error specified.

457 The *neuralnet* package [Fritsch et al. 2016] for the R software was used for the preparation and training of the
458 ANN models. ANN models are able to detect the interactions among the parameters and, since they are not
459 based on a linear combination of the input variables, the transformations proposed for the input variables are no
460 longer necessary either. However, the logarithmic transformations were still applied to the output variables in
461 order to prevent them to reach negative values. Two models were prepared, each of them with one output
462 variable: LS1 and LS3. The ANN model for LS2 was deemed unnecessary because the linear regression model
463 already obtained, shown in Equation (4), was considered accurate enough. The variables used as input are those
464 that proved to be significant predictors of LS1 and LS3 when preparing the multiple linear regression models.
465 This way, the models could also be directly compared. The ANN models have a unique hidden layer with four

466 neurons. This number was determined by a trial and error process. The 10-fold method was used for training and
467 validating the models.

468 The results obtained showed that the ANN models slightly outperformed the multiple linear regression models.
469 Figure 9 shows the predicted versus observed values in both models, showing the improvement in the behavior
470 when compared to the predicted versus observed values obtained for the multiple regression models for LS1
471 (Figure 8a) and LS3 (Figure 7a). The results lie notably closer to the 45° line, even for the highest values of LS1
472 and LS3, which were less accurately estimated by the multiple regression models. Table 4 shows the variables
473 adopted for each regression model and the measurements of performance of both models in terms of errors
474 (MAE and RMSE) and coefficient of determination (R^2). The errors (MAE and RMSE) of the ANN models
475 were reduced around 20% in both models, while the coefficient of determination also increased around 7% for
476 the model predicting the load factor associated with LS1 and 5% for the model predicting the load factor
477 associated with LS3.

478 Besides the aforementioned improvement obtained with the ANN models, they have the disadvantage of not
479 being as straightforward as the MR models. The resulting formulation is not a simple expression such as the
480 ones presented in Equations (2), (3) and (4), but a structure composed of hidden layers, multiple weights and
481 inner functions, as previously explained. Thus, for practical matters, the complexity of the ANN architecture
482 makes the MR models desirable for practical use. They are easy to implement and calculate, while keeping a
483 robust prediction. It is noted that the SAVVAS method is conceived to provide a first seismic assessment that
484 can be carried out in an expedited way, even for large numbers of buildings. Thus, it is preferable that it is based
485 on simple visual inspection and relatively simple formulations.

486 Another main advantage of the multiple regression models is that they are easier to interpret. This is important
487 because the method is also intended to allow performing an initial evaluation of the effect of different
488 retrofitting strategies in reducing the seismic vulnerability of vernacular buildings. Each parameter can be
489 assessed independently directly from Equations (2), (3) and (4), in order to better understand their influence. For
490 instance, the term of Equations (2) involving $P4$ is $(0.186 \times P4)$, where $P4$ refers to the seismic vulnerability
491 class of the building corresponding to the parameter $P4$ (wall-to-wall connections). Thus, the use of a
492 strengthening solution that can improve the wall-to-wall connections and supposes an increase in the seismic

493 vulnerability class from 4 to 1, leads to a quantifiable increase in the maximum capacity of the building (LS3)
494 that can be easily calculated. This increase goes from $e^{(a-0.744)}$ up to $e^{(a-0.186)}$, where a represents the sum of
495 the rest of the terms concerning the other variables and is kept constant, since the strengthening is only applied
496 at the level of the wall-to-wall connections. Since $e^{(a+b)} = e^a \times e^b$, $e^{(-0.744)} = 0.475$ and $e^{(-0.186)} = 0.83$,
497 upgrading the class of P4 from 4 to 1, will suppose a significant increase of LS3, by the order of 1.75 times
498 ($0.83/0.475$). This can be evaluated for every parameter. It also shows that the log transformation of the data
499 adopted seemed to be enough for the multiple regression models to capture adequately the nonlinear
500 relationships and interactions among the variables.

501 **5. Validation of the regression models**

502 The regression models proposed are based on numerical simulations and, sometimes, the accuracy of the
503 regression models might be biased with the intrinsic limitations of the database used for their development,
504 which certainly cannot cover all possible cases. That is why some numerical and experimental studies were
505 gathered from the literature and their results are compared with the model predictions. They consist of six
506 examples of the seismic assessment of different structures that could be associated to the vernacular heritage
507 because of their geometric, construction techniques and material characteristics. The following studies were
508 selected because they provide sufficient information about the buildings to perform the parameter survey and
509 inform about the maximum capacity of the buildings. In this way, the results from the studies can be compared
510 in a straightforward way with the results obtained when applying the regression expressions.

511 As an example of the process of validation followed, the first study consists of a detailed numerical study of the
512 seismic safety analysis of a representative stone masonry structure typology from Lisbon, in Portugal [Mendes
513 and Lourenço 2015]. The buildings belonging to this typology are commonly known as gaioleiro buildings. It
514 represents an appropriate study because the building was studied by means of numerical modeling and pushover
515 analysis, which were the analytical tools also applied for the development of the SAVVAS method.
516 Additionally, the results of the maximum capacity of the building are given in terms of base shear coefficient or
517 load factor, which is the same information that can be obtained after applying the regression equations. Thus,
518 results can be directly compared. Table 5 presents the results obtained in terms of: (1) values adopted for each

519 parameter, according to the attributes necessary to apply the regression models; (2) numerical or experimental
520 seismic coefficient provided by the paper; and (3) the estimated load factor associated to LS3 obtained using
521 two different regression models.

522 It should be highlighted that the regression models also allow to distinguish the seismic behavior of the building
523 in the four principal directions (+/-X and +/-Y), which is not possible using other simplified formulations. Since
524 the value of most parameters depends on the evaluated direction, assessing each resisting direction leads to
525 different values of the maximum capacity. This is in agreement with the reviewed study, which revealed that the
526 capacity of the building is very different in each principal direction (X and Y). This feature is well-captured by
527 the SAVVAS regression models which shows a good correlation between the numerical seismic coefficient
528 from the paper and the predicted load factor obtained from the method. The reviewed paper also included a
529 parametric analysis that consists of varying the material properties of the masonry walls. The results of this
530 parametric study were also correlated with the results obtained from the regression models modifying parameter
531 P3, assuming varying material quality of the masonry walls. The change in the material properties is indicated in
532 Table 5 with (+) when they were increased and with (-) when they were reduced. A very good correlation
533 between the results from the paper and the predicted load factor can be highlighted. The method is thus able to
534 simulate accurately the variations in the parametric analysis simply by increasing or decreasing one
535 vulnerability class in P3. Both models (MR and ANN) provide a good accuracy with a maximum difference of
536 0.08g.

537 Another example consists of the validation of the regression models with the results of another experimental test
538 conducted at the EUCENTRE research center in Pavia, Italy [Magenes et al. 2014]. The test campaign consisted
539 on shaking table tests on two full-scale two-story unreinforced masonry buildings with timber floors. The first
540 prototype was an unstrengthened reference prototype (URM) without seismic resistant detailing, while the
541 second specimen introduced some reinforcement measures (RM). In this case, only the results of the
542 experimental campaign are available, so the results of the method were compared with the maximum resisted
543 base shear coefficient.

544 Even though detailed information about the construction of the two specimens is given in the paper, some of the
545 qualitative parameters have to be assumed by the photos or by the descriptive qualitative information provided.

546 For example, for the URM building, the type of horizontal diaphragm is considered as class D. According to the
547 plans shown in the paper, the beams are only connected to the walls by a partial embedment within the wall but
548 there is no strengthened connection between the floor sheathing and the walls. This class was upgraded to class
549 B for the RM buildings, since the strengthening interventions were destined to improve the wall-to-floor and
550 wall-to-roof connections and to moderately improve the in-plane stiffness of the floor, aimed at preventing the
551 occurrence of premature out-of-plane failure mechanisms. The undressed double-leaf stone masonry of the walls
552 is considered as class B because of the assumed good workmanship at the laboratory. Also, the authors report
553 that some damage took place on the RM building during the transportation phase, with observed cracks below 1
554 mm. Thus, a class B on the previous structural damage (P9) was adopted.

555 The regression models predict very accurately the maximum capacity of the building and capture very well the
556 improvement in the seismic behavior when applying the strengthening intervention in the floors. Table 6 shows
557 that the errors in the prediction of the multiple linear regression models are below 0.03g. Even though the
558 uniaxial shaking table only imposed the base motion in +/- X direction, the performance of the building was
559 evaluated in all directions, including +/-Y, because the regression models can estimate the weakest direction of
560 the building. Thus, it is interesting to see how the method predicts that the unreinforced building, which is prone
561 to out-of-plane collapse, is more vulnerable in Y direction while, after the intervention in the diaphragms, the
562 building is more likely to fail in X direction. The method is thus able to show that reinforcing the diaphragms
563 will have an effect in the failure mode of the building, leading to the development of in-plane resisting
564 mechanisms. This change in the failure mode was also reported in the reviewed paper.

565 A third example consisted of the application of the regression models to a study conducted at EUCENTRE
566 research center in Pavia, Italy, consisting of a unidirectional shaking table test of a full-scale unreinforced clay
567 brick masonry building [Kallioras et al. 2018]. The study provides the results of the experimental campaign in
568 terms of maximum accelerations measured in g, which were compared with the results obtained after the
569 application of the regression models. The paper provided information about the base-shear coefficients (*BSC*)
570 that led the building to reach different damage states, including: (a) the *BSC* corresponding to the onset of the
571 first significant cracks, which can be correlated with the load factor related to the reaching of LS1; and (b) the
572 maximum attained overall *BSC* for the building, which can be correlated with the load factor related to the

573 reaching of LS3. Thus, the two regression models aimed at the estimation of the load factors associated with
574 LS1 and LS3 could be used and the results compared with the ones observed experimentally, see Table 7.
575 Results for all limit states show a good agreement between the predicted values with the multiple regression
576 models and the experimentally obtained values, with minimum errors, validating the results obtained with the
577 two regression expressions. Errors are slightly higher for the ANN models.

578 The remaining three case studies consists of: (1) an experimental campaign carried out on a two-story
579 unreinforced stone masonry building that was tested on a shaking table test at the CNR-ENEA research center
580 of Casaccia, in Rome, Italy [Betti et al. 2014]. The results of the experimental analysis were replicated with
581 finite element modelling and pushover analysis. These numerical results were compared with the results
582 obtained after the application of the regression equations from the SAVVAS method; (2) an experimental
583 campaign carried out at the LEE/NTUA research center in Athens, Greece [Mouzakis et al. 2012], where two
584 reduced scaled (1:2) two-story stone masonry buildings were tested on a bi-directional shaking table: one
585 unstrengthened reference prototype (URM) and a second specimen with some reinforcement measures (RM).
586 This study also just provides the results of the experimental campaign and thus the results obtained after the
587 application of the regression models were compared with the values of maximum accelerations measured in g
588 given by the paper; and (3) an experimental campaign of two-story unreinforced stone and brick masonry
589 buildings tested on a shaking table by ISMES, in Bergamo, Italy and LEE/NTUA, in Athens, Greece [Benedetti
590 et al. 1998]. The results obtained from the test on a stone masonry specimen (STM) and a brick specimen (BM)
591 are provided in terms of maximum lateral force coefficients so they can be compared with the results provided
592 after the application of the SAVVAS regression models.

593 As a summary, Table 8 provides the most relevant results obtained for the validation of the regression models.
594 All the results correspond to the load factor associated with LS3 because it could be calculated in the six cases.
595 The prediction capability of the models was considered validated, given the low errors obtained, particularly for
596 the multiple regression models. The regression models are also able to detect the most vulnerable direction of
597 the buildings and simulate well the effect of the reinforcing techniques.

598 **6. SAVVAS formulation**

599 The prediction capability of the regression models was considered validated with the examples available in the
600 literature, given the low errors obtained, particularly for the multiple regression models. This confirmed also the
601 potential of the method and, consequently, a final formulation for the SAVVAS method is proposed using the
602 expressions for the three limit states shown in Equations (2), (3) and (4). Table 9 summarizes the process and
603 provides the final formulation of the SAVVAS method. As observed during the validation process, the
604 application of the method simply consists of three steps: (1) collection of the data related to the ten key seismic
605 vulnerability assessment parameters, defined either by specifying different quantitative attributes or by
606 assigning a seismic vulnerability class from 1 to 4; (2) application of the regression models expressions to
607 determine the three different values of load factor defining each limit state (LS1, LS2 and LS3). With the
608 obtainment of these values, it is possible to have an estimation of the seismic actions that can cause the building
609 to reach the different structural limit states for each direction, expressed as an acceleration (in terms of g); and
610 (3) estimation of the minimum load that will cause the building to reach the different limit states. Since this
611 method allows calculating a different load factor in each main direction of the building, the load factor
612 representing the global vulnerability of the building is defined as the minimum value obtained among the four
613 resisting directions. Moreover, since the load factors related with the different structural damage limit states are
614 expressed as accelerations, they can be used in a straightforward way to eventually correlate the seismic action
615 in terms of peak ground acceleration (PGA) with the expected damage. Alternatively, as previously stated, when
616 a more refined assessment is required, the site response spectra and the building fundamental period can be used
617 to take into account specific accelerations adapted to each building and site.

618 **7. Final considerations**

619 The main objective of the present paper has been the presentation and validation of the numerical tool that
620 constitute the core of a new method for the seismic vulnerability assessment of vernacular architecture, referred
621 as Seismic Assessment of the Vulnerability of Vernacular Architecture Structures (SAVVAS). The method is
622 intended to be an expedited simplified approach that provides the possibility of performing a primary seismic
623 safety assessment of a vernacular building or group of buildings based on simple surveys that can be carried out

624 even solely by means of visual inspection. These methods are particularly appropriate when addressing large
625 number of buildings or when the necessary amount of resources required in order to perform more sophisticated
626 analyses cannot be assigned to the assessment of the targeted buildings, which is generally the case when
627 dealing with the study of vernacular constructions.

628 The SAVVAS method is considered innovative method because it provides a new formulation that allows
629 defining the seismic capacity of the building through seismic load factors associated with different damage limit
630 states using simple parameters and classes typically used in classical simplified seismic vulnerability index
631 methods. Since these load factors expressed as accelerations (in terms of g) are related with structural damage
632 limit states, the SAVVAS method is intended to directly correlate accelerations induced by the seismic event
633 with the expected damage. For that matter, we can use as seismic input the peak ground acceleration (PGA) for
634 a simplified assessment or we can use the site response spectra and the building natural frequency for a more
635 detailed assessment that uses specific accelerations adapted to each building and site. This is one main
636 advantage of the SAVVAS method over more classical seismic vulnerability index approaches. Vulnerability
637 index formulations calculate a vulnerability index (I_v), which is just an intermediate step to estimate the damage
638 suffered by a building under an earthquake of a specific intensity, because empirically developed expressions
639 have to be later implemented to correlate I_v with damage. The vulnerability functions resulting from the
640 SAVVAS method are able to directly relate the seismic accelerations with structural limit states and,
641 subsequently, with expected damage. This correlation is necessary in order to perform damage and loss
642 assessments.

643 Even though the parameters selection was done through a combination of empirical observation and expert
644 judgment, this method is considered analytical in its development because it relies on a solid numerical
645 parametric study. The influence of the different parameters was validated through detailed finite element
646 modeling and pushover analysis. Results helped to obtain a comprehensive understanding of the seismic
647 behavior of vernacular architecture and to provide a quantitative definition of seismic vulnerability classes. The
648 use of an analytical procedure for the definition of the seismic vulnerability assessment classes helps to
649 strengthen the reliability of the existing simplified methods that typically rely solely on empirical knowledge
650 obtained from post-earthquake damage observation.

651 In a second step, data mining (DM) techniques were applied on the database resulting from the numerical
652 campaign. The primary goal was to obtain regression models able to predict the load factors corresponding to
653 different structural limit states using as predictors variables associated to the seismic vulnerability assessment
654 parameters previously defined. Several multiple regression and ANN models were developed and proved to be
655 reliable in their predictive capabilities. The development of the models also allowed a better understanding of
656 the role of the seismic vulnerability parameters on defining the seismic response of vernacular buildings and
657 helped to discover complex relationships among them. The regression models were validated with their
658 application on numerical and experimental examples found in the literature, revealing a very good correlation
659 between the predicted and observed seismic load factor. During this validation process, they were also
660 confirmed to be useful in assessing the effect of some reinforcement techniques on the final seismic capacity of
661 the building. Moreover, they also provide information about the capacity of the building in each main direction,
662 which is another advantage of this method because it allows identifying the weakest direction and possible
663 failure mechanisms. Thus, it can be of great help in identifying deficiencies of the structure before making
664 decisions on strengthening interventions.

665 The robustness of the regression models is conditioned by the limitations and assumptions existing in nonlinear
666 static analysis of masonry and earthen vernacular buildings. The results obtained when applying the regression
667 expressions would simulate the results obtained as if we were performing a pushover analysis on a structure
668 with such characteristics. The method is also conditioned by the size of the database which, even though is
669 considered exhaustive, cannot comprehend the vast amount of possibilities observed in vernacular buildings. It
670 should be here noted that, in any case, the database used can always be further enlarged with more results in
671 order to make it more comprehensive. The SAVVAS formulation and procedure have been defined but the
672 database remains open for future extension. Nonetheless, the results obtained with the current form are deemed
673 satisfactory, since the models are able to provide a reliable first estimate of the seismic capacity of a building
674 based solely on limited information related to the ten key seismic vulnerability parameters.

675

676 **References**

- 677 Aguilar V, Sandoval C, Adam JM, Garzón-Roca J, Valdebenito G (2016) Prediction of the shear strength of
678 reinforced masonry walls using a large experimental database and artificial neural networks, *Structure and*
679 *Infrastructure Engineering* 12 (12): 1661-1674
- 680 Angulo-Ibáñez Q, Mas-Tomás Á, Galvañ-Llopis V, Sántolaria-Montesinos JL (2012) Traditional braces of earth
681 constructions. *Constructions and Building Materials* 30: 389-399
- 682 Barbat A, EERI M, Yépez Moya F, Canas JA (1996) Damage Scenarios Simulation for Seismic Risk
683 Assessment in Urban Zones, *Earthquake Spectra* 12 (3): 371-394
- 684 Baykasoglu A, Güllü H, Çanakçı H, Özbakir L (2008) Prediction of compressive and tensile strength of
685 limestone via genetic programming, *Expert Systems with Applications* 35: 111-123
- 686 Benedetti D, Petrini V (1984) Sulla Vulnerabilità Di Edifici in Muratura: Proposta Di Un Metodo Di
687 Valutazione, *L'industria delle Costruzioni* 149 (1): 66-74
- 688 Benedetti D, Carydis P, Pezzoli P (1998) Shaking table tests on 24 simple masonry buildings, *Earthquake*
689 *Engineering and Structural Dynamics* 27: 67-90
- 690 Betti M, Galano L, Vignoli A (2014) Comparative analysis on the seismic behaviour of unreinforced masonry
691 buildings with flexible diaphragms, *Engineering Structures* 61: 195-208
- 692 Blondet M, Villa García GM, Brzev S, Rubiños A (2011) Earthquake-resistant construction of adobe buildings:
693 a tutorial, Earthquake Engineering Research Institute (EERI), Oakland, California, USA
- 694 Bothara J, Brzev S (2012) A tutorial: improving the seismic performance of stone masonry buildings,
695 Earthquake Engineering Research Institute (EERI), Oakland, California, USA
- 696 Boukri M, Bensaibi M (2008) Vulnerability Index of Algiers Masonry Buildings, in: Proc. of 14th World
697 Conference on Earthquake Engineering, Beijing, China
- 698 Correia M (2002) A habitação vernácula rural no Alentejo, Portugal, in: Memórias del IV Seminario
699 Iberoamericano sobre vivienda rural y calidad de vida en los asentamientos rurales, Santiago del Chile, Chile

700 Correia M (2007) Taipa no Alentejo, Argumentum, Lisboa, Portugal

701 Correia M (2017) Experiences from past for today's challenges, in: The road to sustainable development.
702 Chapter 6 – Traditional and generational change, La fábrica, Fundación Contemporánea, Madrid, Spain

703 Cortez P (2010) Data Mining with Neural Networks and Support Vector Machines Using the R/rminer Tool, in:
704 Proc. of 10th Industrial Conference, ICDM 2010, Berlin, Germany

705 Degg MR, Homan J (2005) Earthquake vulnerability in the Middle East, *Geography* 90 (1): 54-66

706 EN 1998-3 (2005) Eurocode 8: Design of structures for earthquake resistance – Part 3: Assessment and
707 retrofitting of buildings. CEN, Brussels, Belgium

708 Fayyad U, Piatetsky-Shapiro G, Smyth P (1996) From Data Mining to Knowledge Discovery in Databases, *AI*
709 *Magazine* 17 (3): 37-54

710 Ferreira TM, Vicente R, Mendes da Silva JAR, Varum H, Costa A (2013) Seismic vulnerability assessment of
711 historical urban centres: case study of the old city centre in Seixal, Portugal, *Bulletin of Earthquake Engineering*
712 11 (5): 1753-1773

713 Ferreira TM, Vicente R, Varum H (2014) Seismic vulnerability assessment of masonry facade walls:
714 development, application and validation of a new scoring method, *Structural Engineering and Mechanics* 50 (4):
715 541-561

716 Field A, Miles J, Field Z (2012) *Discovering Statistics Using R*, SAGE Publishing

717 Fritsch S, Günther F, Suling M, Müller S (2016) Package 'neuralnet', R manual

718 Gallego R, Arto I (2014) Evaluation of seismic behaviour of rammed earth structures, in: Mileto, Vegas,
719 Soriano & Cristini (eds), *Earthen architecture: past, present and future*, Taylor & Francis Group, London, UK

720 Garzón-Roca J, Marco C, Adam JM (2013a) Compressive strength of masonry made of clay bricks and cement
721 mortar: Estimation based on neural networks and fuzzy logic, *Engineering Structures* 48: 21-27

722 Garzón-Roca J, Adam JM, Sandoval C, Roca P (2013b) Estimation of the axial behavior of masonry walls
723 based on artificial neural networks, *Computers and Structures* 125: 145-152

724 Gautam D, Prajapati J, Paterno KV, Bhetwal KK, Neupane P (2016) Disaster resilient vernacular housing
725 technology in Nepal, *Geoenvironmental Disasters* 3 (1)

726 GNDT (1994) Scheda di esposizione e vulnerabilita ` e di rilevamento danni di primo livello e secondo livello
727 (muratura e cemento armato), Gruppo Nazionale per la Difesa dai Terremoti (GNDT), Rome, Italy

728 Gomes MI, Lopes M, de Brito J (2011) Seismic resistance of earth construction in Portugal, *Engineering*
729 *Structures* 33 (3): 932-941

730 Günther F, Fritsch S (2010) neuralnet: Training of Neural Networks, *The R Journal* 2 (1): 30-38

731 ICOMOS (1999) Charter on the built vernacular heritage, International Council of Monuments and Sites
732 (ICOMOS), ICOMOS 12th General Assembly, Mexico

733 Kallioras S, Guerrini G, Tomassetti U, Marchesi B, Penna A, Graziotti F (2018) Experimental seismic
734 performance of a full-scale unreinforced clay-masonry building with flexible timber diaphragms, *Engineering*
735 *Structures* 161: 231-249

736 Karanikoloudis G, Lourenço PB (2018) Structural assessment and seismic vulnerability of earthen historic
737 structures. Application of sophisticated numerical and simple analytical models, *Engineering Structures* 160:
738 488-509

739 Kottegodo N, Rosso R (2008) *Applied Statistics for Civil and Environmental Engineers*, Blackwell Publishing,
740 New Jersey, USA

741 Lourenço PB (2009) Recent advances in masonry structures: micromodelling and homogenization, in:
742 Galvanetto & Ferri Aliabadi (eds), *Multiscale modeling in solid mechanics: computational approaches*, pp. 280-
743 300, Imperial College Press, London, UK

744 Lourenço PB, Mendes N, Ramos LF, Oliveira DV (2011) Analysis of masonry structures without box-behavior,
745 *International Journal of Architectural Heritage. Conservation, Analysis and Restoration* 5 (4-5): 369-382

746 Lourenço PB, Karanikoloudis G, Mendes N, Corallo C (2015) Assessment of the South aisle in Canterbury, in:
747 *Proc. of the 2nd International conference on preservation, maintenance and rehabilitation of historical buildings*
748 *and structures*, Porto, Portugal

749 Magenes G, Penna A, Senaldi IE, Rota M, Galasco A (2014) Shaking Table Test of a Strengthened Full-Scale
750 Stone Masonry Building with Flexible Diaphragms, *International Journal of Architectural Heritage.*
751 *Conservation, Analysis and Restoration* 8: 349-375

752 Mallardo V, Malvezzi R, Milani E, Milani G (2008) Seismic vulnerability of historical masonry buildings: a
753 case study in Ferrara, *Engineering Structures* 30: 2223-2241

754 Marques R, Lourenço PB (2013) A model for pushover analysis of confined masonry structures:
755 implementation and validation, *Bulletin of Earthquake Engineering* 11: 2133-2150

756 Martins F, Vasconcelos G, Miranda T (2014) The performance of ultrasonic pulse velocity on the prediction of
757 tensile granite behaviour: a study based on artificial neural networks, in: *Proc. of 9th International Masonry*
758 *Conference, Guimarães, Portugal*

759 Martins F, Vasconcelos G, Miranda T (2018) Prediction of the mechanical properties of granite under tension
760 using DM techniques, *Geomechanics and Engineering* 15(1): 631-643

761 May J (2010) *Handmade houses & other buildings: the world of vernacular architecture*, Thames & Hudson,
762 London, UK

763 Mendes N, Lourenço PB (2010) Seismic assessment of masonry ‘Gaioleiro’ buildings in Lisbon, Portugal,
764 *Journal of Earthquake Engineering* 14: 80-101

765 Mendes N, Lourenço PB (2015) Seismic vulnerability of existing masonry buildings: nonlinear parametric
766 analysis, in: Psycharis, Pantazopoulou & Papadrakakis (eds), *Seismic assessment, behavior and retrofit of*
767 *heritage buildings and monuments. Computational methods in applied sciences*, Vol. 37, Springer

768 McCune B, Graces J (2002) *Analysis of Ecological Communities*, MjM Software Design, Gleneden, USA

769 Miccoli L, Oliveira DV, Silva R, Müller U, Schueremans L (2014) Static behaviour of rammed earth:
770 experimental testing and finite element modelling, *Materials and Structures* 48 (10): 3443-3456

771 Miranda T, Correia AG, Santos M, Ribeiro e Sousa L, Cortez P (2011) New Models for Strength and
772 Deformability Parameter Calculation in Rock Masses Using Data-Mining Techniques, *International Journal of*
773 *Geomechanics* 11 (1): 44-58

774 Montgomery DC, Peck EA, Vining GG (2012) Introduction to linear regression analysis, John Wiley & Sons,
775 Inc., New Jersey, USA

776 Mouyiannou A, Rota M, Penna A, Magenes G (2014) Identification of suitable limit states from nonlinear
777 dynamic analyses of masonry structures, *Journal of Earthquake Engineering* 18 (2): 231-263

778 Mouzakis C, Vintzileou E, Adam CE, Karapitta L (2012) Dynamic tests on three leaf stone masonry building
779 model before and after interventions, in: *Proc. of Structural Analysis of Historical Constructions, SAHC 2012*,
780 Wroclaw, Poland

781 Neves F, Costa A, Vicente R, Oliveira CS, Varum H (2012) Seismic vulnerability assessment and
782 characterization of the buildings on Faial Island, Azores, *Bulletin of Earthquake Engineering* 10 (1): 27-44

783 NTC (2008) Norme Tecniche per le Costruzioni. D.M. 14 gennaio 2008, S.O. No. 30, G.U. No. 29/2008, Rome,
784 Italy

785 Oliver P (1997) *Encyclopedia of vernacular architecture of the world*, Cambridge University Press, Cambridge,
786 UK

787 Ortega J, Vasconcelos G, Rodrigues H, Correia M (2018) Assessment of the efficiency of traditional earthquake
788 resistant techniques for vernacular architecture, *Engineering Structures* 173

789 Ortega J (2018) Reduction of the seismic vulnerability of vernacular architecture with traditional strengthening
790 solutions, Ph.D. thesis, University of Minho, Guimarães, Portugal

791 Plevris V, Asteris PG (2014) Modeling of masonry failure surface under biaxial compressive stress using neural
792 networks, *Construction and Building Materials* 55: 447-461

793 R Development Core Team (2008) *R: A language and environment for statistical computing*, R Foundation for
794 Statistical Computing, Vienna, Austria

795 Rapoport A (1969) *House, form and culture*, Prentice-Hall, Englewoods Cliffs, USA

796 Rota M, Penna A, Magenes G (2010) A methodology for deriving analytical fragility curves for masonry
797 buildings based on stochastic nonlinear analyses, *Engineering Structures* 32: 1312-1323

798 Rudofsky B (1964) Architecture without architects – a short introduction to non-pedigreed architecture,
799 Museum of Modern Art, New York, USA

800 Saloustros S, Pelà L, Roca P, Portal J (2014) Numerical analysis of structural damage in the church of the
801 Poblet Monastery, Engineering Failure Analysis 48: 41-61

802 Sandoval C, Roca P (2012) Study of the influence of different parameters on the buckling behaviour of masonry
803 walls, Construction and Building Materials 35: 888-899

804 Shakya M (2014) Seismic vulnerability assessment of slender masonry structures, Ph.D. thesis, Universidade de
805 Aveiro, Aveiro, Portugal

806 Sorrentino L, Liberatore L, Liberatore D, Masiani R (2013) The behaviour of vernacular buildings in the 2012
807 Emilia earthquakes, Bulletin of Earthquake Engineering 12(5): 2367-2382

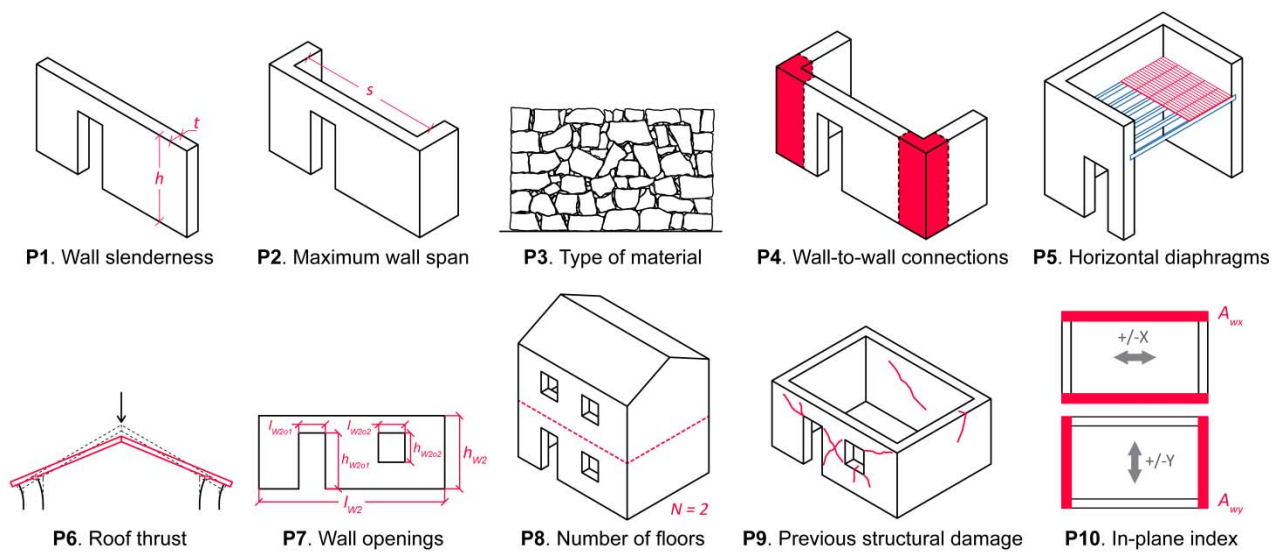
808 Sepe V, Speranza E, Viskovic A (2008) A method for large-scale vulnerability assessment of historic towers,
809 Journal of Structural Control and Health Monitoring 15: 389-415

810 TNO (2011) DIsplacement method ANAlyser. User's manual, release 9.4.4., Netherlands

811 Vicente R (2008) Estratégias e metodologias para intervenções de reabilitação urbana. Avaliação da
812 vulnerabilidade e do risco sísmico do edificado da Baixa de Coimbra, Ph.D. thesis, Universidade do Aveiro,
813 Aveiro, Portugal

814 Vicente R, Parodi S, Lagomarsino S, Varum H, Mendes da Silva JAR (2011) Seismic vulnerability and risk
815 assessment: a case study of the historic city centre of Coimbra, Portugal, Bulletin of Earthquake Engineering 9
816 (4): 1067-1096

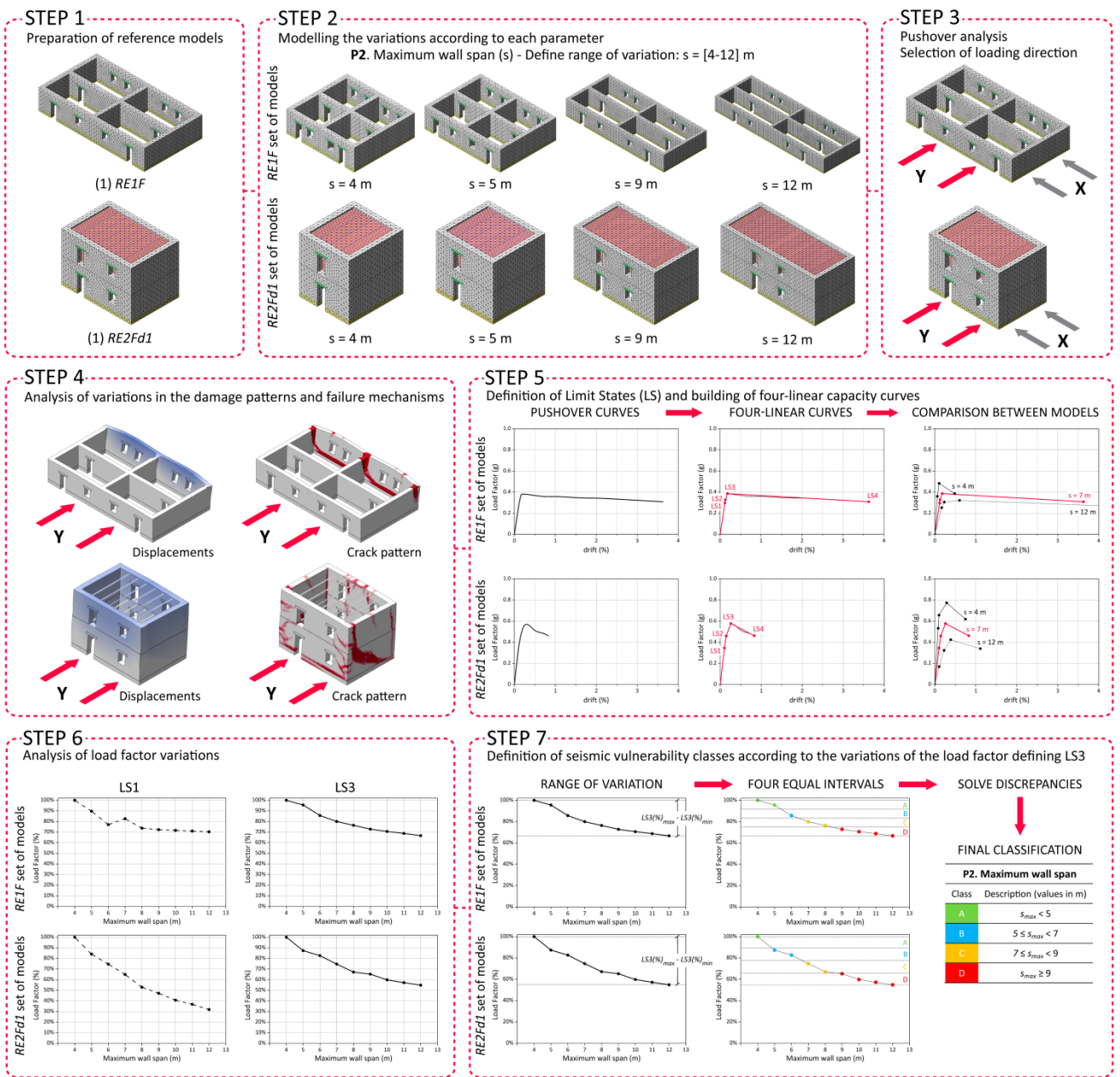
817



818

819 Figure 1. Seismic vulnerability assessment parameters considered for the SAVVAS method

820



821

822 Figure 2. Seven steps followed for the definition of the seismic vulnerability classes using parameter P2

823 (maximum wall span) as an example

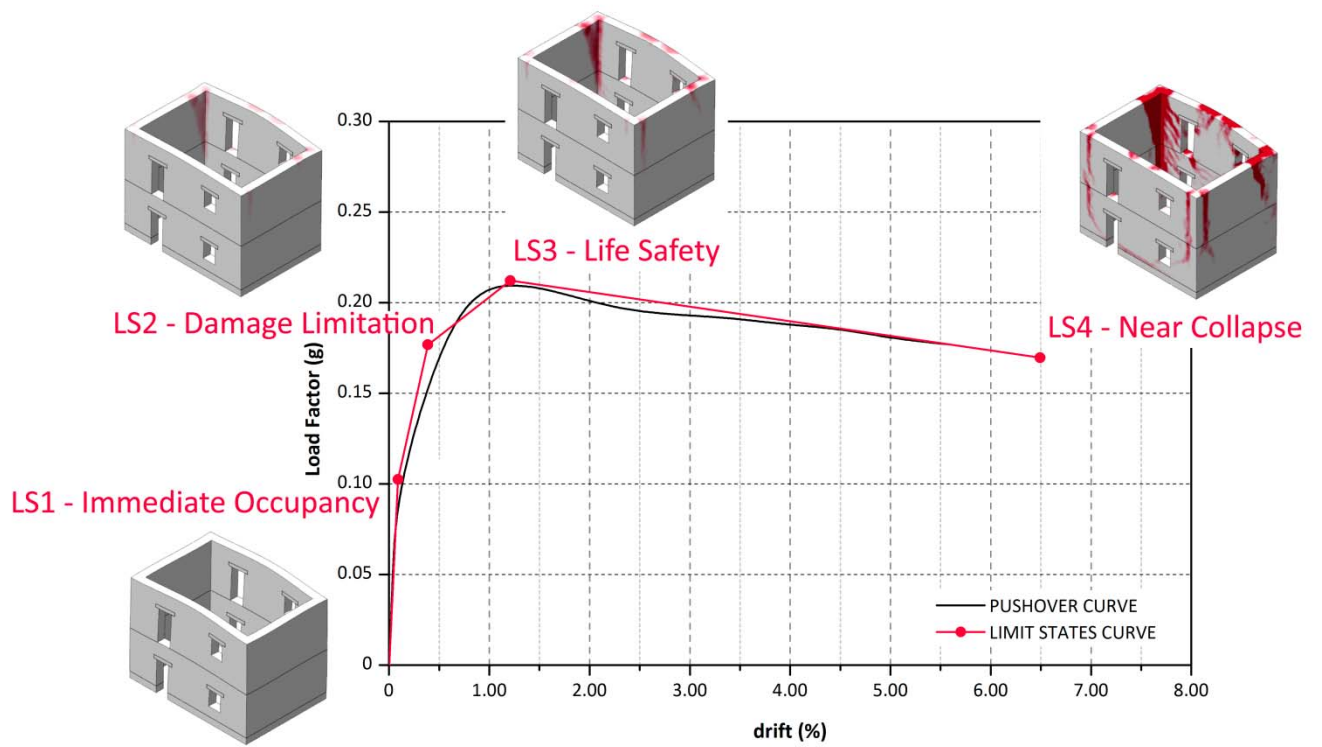
824



825

826 Figure 3. Examples of vernacular buildings targeted by the SAVVAS method in Portugal: (a) stone masonry
827 buildings in Vila Real de Santo António historic city center; (b) adobe masonry rural construction in Alentejo
828 [Correia 2002]; (c) rammed earth urban building in Serpa [Correia 2002]; (d) stone masonry buildings in Lagos
829 historic city center; and (e) rammed earth rural construction in Alcácer do Sal [Correia 2007]

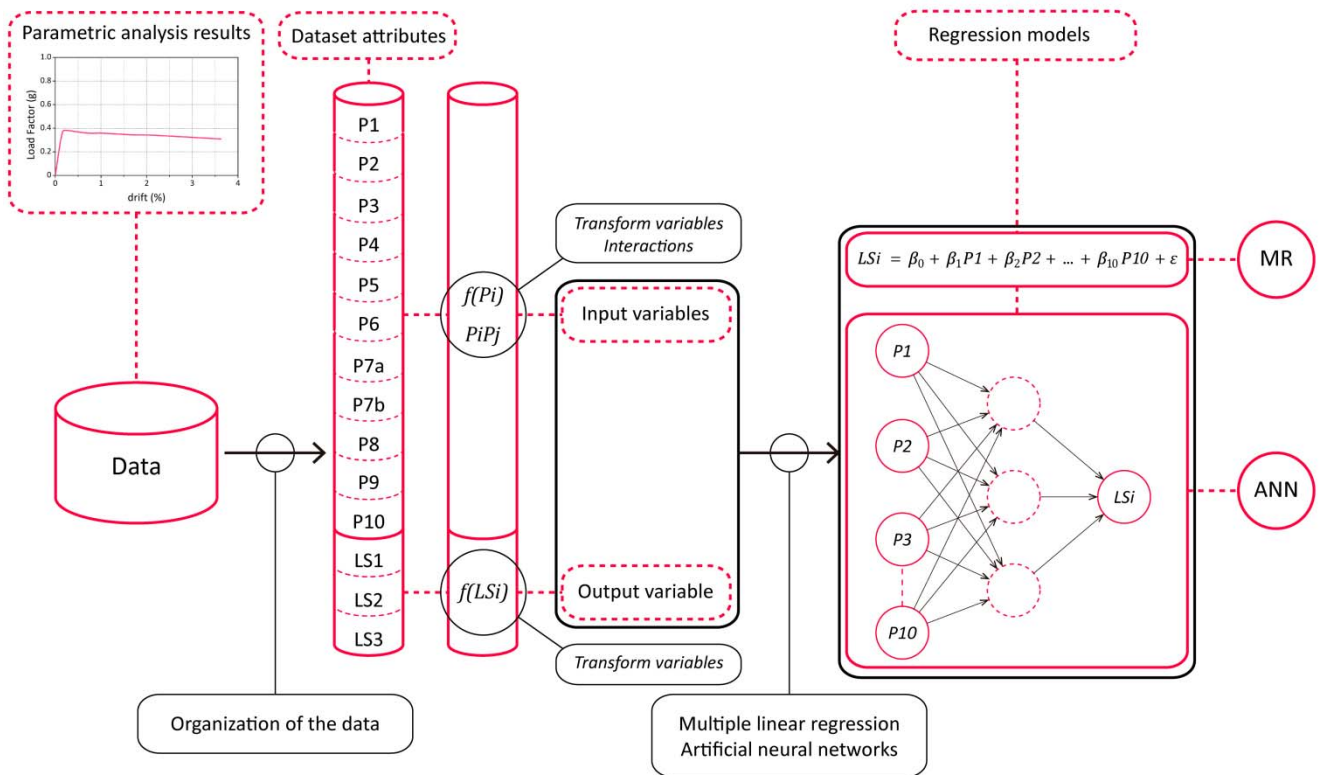
830



831

832 Figure 4. Definition of the four limit states according to the pushover curve

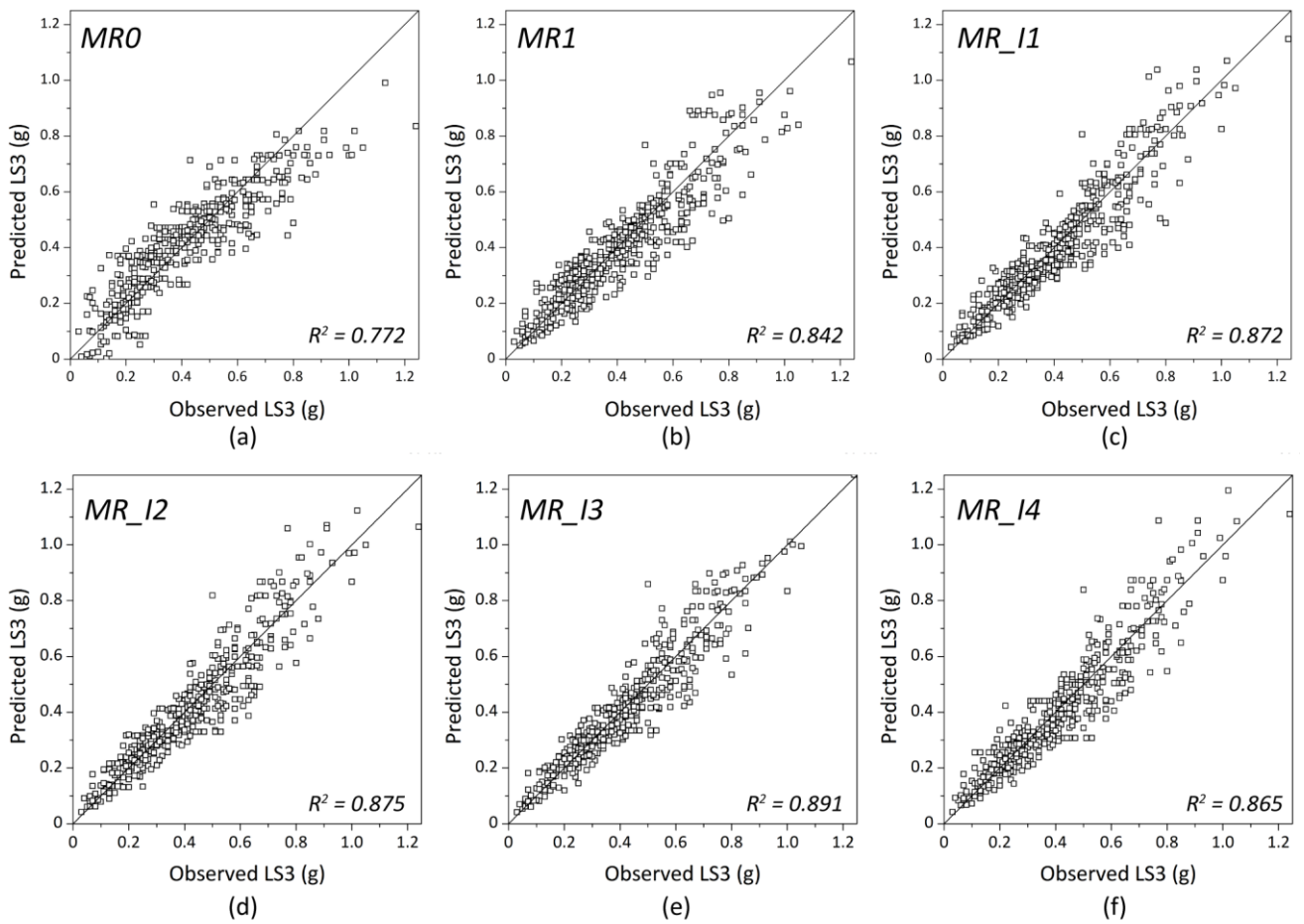
833



834

835 Figure 5. Methodology adopted **to obtain the regression models of** the SAVVAS method

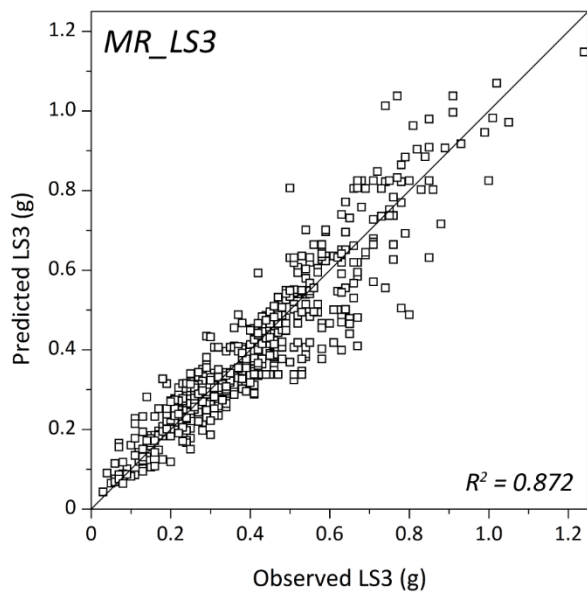
836



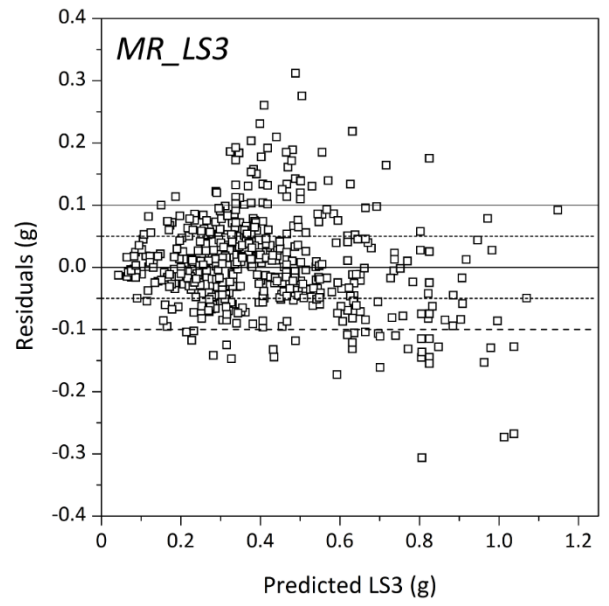
837

838 Figure 6. Comparison of predicted versus observed values for the six regression models constructed

839



(a)

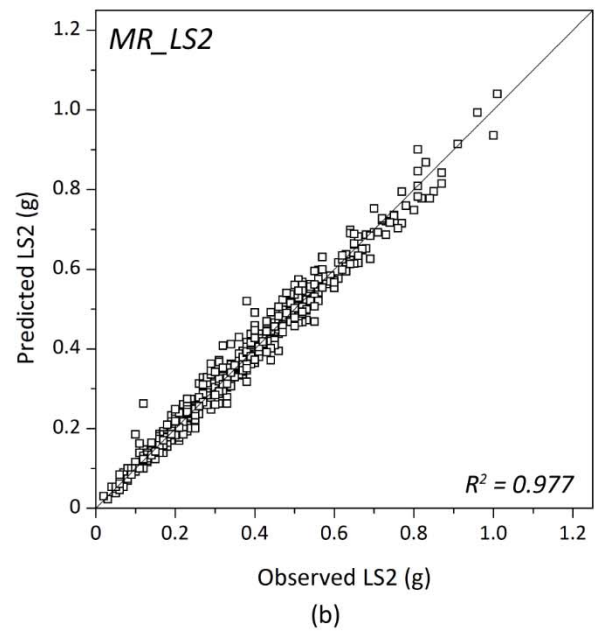
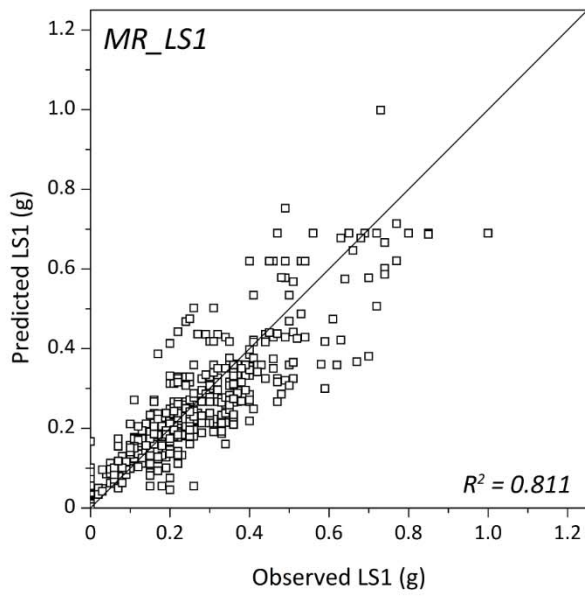


(b)

840

841 Figure 7. (a) Predicted versus observed values for the *MR_LS3* model; and (b) residual versus fitted values

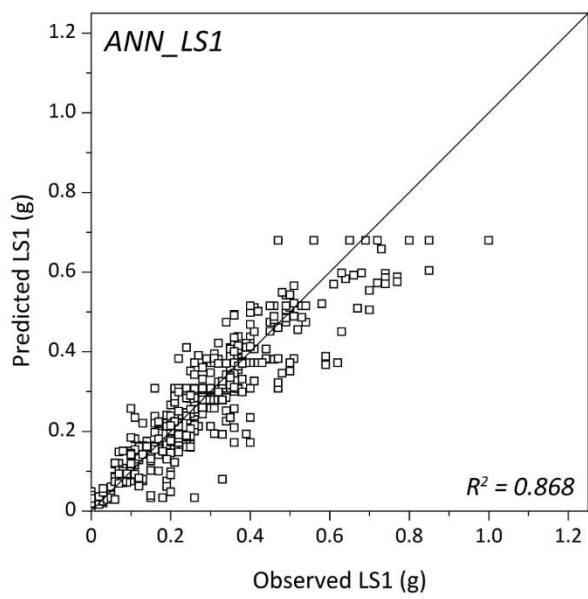
842



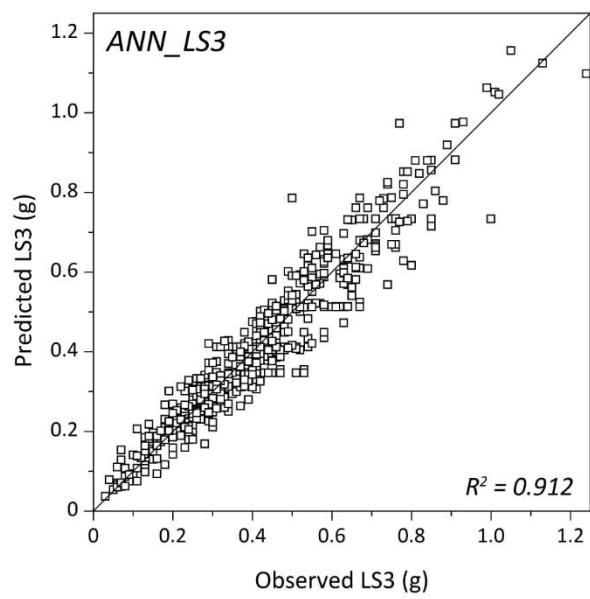
843

844 Figure 8. Predicted versus observed values for: (a) *MR_LS1* model; and (b) *MR_LS2* model

845



(a)



(b)

846

847 Figure 9. Predicted versus observed values for: (a) *ANN_LS1* model; and (b) *ANN_LS3* model

848

849 Table 1. List of variables and general statistical measures

| Variables | | Description | Minimum | Maximum | Mean | Median | Mode | STD |
|---------------|------------------|--|---------|---------|-------|--------|-------|------|
| P1 | λ | Ratio between the effective wall inter-story height (h) and its thickness | 4 | 22.5 | 7.34 | 6 | 5.6 | 3.43 |
| | $\lambda^{-1/2}$ | Power transformation of the variable | 0.21 | 0.50 | 0.39 | 0.41 | 0.42 | 0.06 |
| P2 | s | Maximum wall span without intermediate supports, measured in meters (m) | 2.5 | 12 | 5.90 | 5.25 | 7 | 1.87 |
| | $\ln(s)$ | Log transformation of the variable | 0.92 | 2.48 | 1.73 | 1.66 | 1.95 | 0.30 |
| P3 | $P3$ | Seismic vulnerability class of the building according to P3 | 1 | 4 | 3.36 | 4 | 4 | 1.04 |
| | $\ln(P3)$ | Log transformation of the variable | 0 | 1.39 | 1.14 | 1.39 | 1.39 | 0.44 |
| P4 | $P4$ | Seismic vulnerability class of the building according to P4 | 1 | 4 | 1.44 | 1 | 1 | 0.94 |
| P5 | $P5$ | Seismic vulnerability class of the building according to P5 | 1 | 4 | 2.71 | 3 | 4 | 1.38 |
| | $\ln(P5)$ | Log transformation of the variable | 0 | 1.39 | 0.82 | 1.10 | 1.39 | 0.64 |
| P6 | $P6$ | Seismic vulnerability class of the building according to P6 | 1 | 4 | 1.24 | 1 | 1 | 0.70 |
| | $P7a$ | Ratio between the maximum area of wall openings in a wall perpendicular to the loading direction and the total area of the considered wall | 0 | 0.7 | 0.09 | 0.06 | 0 | 0.16 |
| P7 | $P7b$ | Ratio between the area of wall openings in all in-plane resisting walls and the total area of all in-plane resisting walls | 0 | 0.69 | 0.12 | 0 | 0 | 0.18 |
| | N | Number of floors | 1 | 4 | 1.87 | 2 | 1 | 0.89 |
| P8 | $\ln(N)$ | Log transformation of the variable | 0 | 1.39 | 0.51 | 0.69 | 0 | 0.47 |
| | $P9$ | Seismic vulnerability class of the building according to P9 | 1 | 4 | 1.29 | 1 | 1 | 0.77 |
| P9 | $\ln(P9)$ | Log transformation of the variable | 0 | 1.39 | 0.15 | 0 | 0 | 0.39 |
| | $P10$ | Ratio between the in-plan area of earthquake resistant walls in the loading direction and the total in-plan area of earthquake resistant walls | 0.26 | 0.79 | 0.53 | 0.50 | 0.50 | 0.11 |
| Output | LS1 (g) | $LS1(g)$ | 0 | 1 | 0.24 | 0.23 | 0 | 0.18 |
| | | $\ln(LS1+c)$ | -4.61 | 0.01 | -1.86 | -1.43 | -4.61 | 1.28 |
| | LS2 (g) | $LS2(g)$ | 0.02 | 1.01 | 0.36 | 0.35 | 0.38 | 0.19 |
| | | $\ln(LS2)$ | -3.91 | 0.01 | -1.17 | -1.05 | -0.97 | 0.62 |
| | LS3 (g) | $LS3(g)$ | 0.03 | 1.24 | 0.42 | 0.41 | 0.41 | 0.21 |
| | | $\ln(LS3)$ | -3.51 | 0.22 | -1.02 | -0.89 | -0.89 | 0.59 |

850

851

852 Table 2. Different regression models constructed with measurements of their performance

| Model | Variables | | Interactions | R ² | ϵ_{max} | MAE | RMSE |
|-------|-----------|---|---|----------------|------------------|--------|--------|
| | Output | Input | | | | | |
| MR0 | LS3 | P1; P2; P3; P4; P5; P6; P7; P8; P9; P10 | - | 0.772 | 0.405g | 0.075g | 0.095g |
| MR1 | ln(LS3) | λ ; s; P3; P4; P5; P6; P7a; P7b; N; P9; γ_i | - | 0.842 | 0.296g | 0.064g | 0.084g |
| MR_11 | ln(LS3) | λ ; s; P3; P4; P5; P6; P7a; P7b; N; P9; γ_i | P5:P7b | 0.872 | 0.318g | 0.057g | 0.078g |
| MR_12 | ln(LS3) | $\lambda^{-1/2}$; ln(s); ln(P3); P4; P5; P6; P7a; P7b; ln(N); ln(P9); γ_i | P5:P7b P7b:ln(N) | 0.875 | 0.320g | 0.056g | 0.076g |
| MR_13 | ln(LS3) | $\lambda^{-1/2}$; ln(s); ln(P3); P4; P5; ln(P5); P6; P7a; P7b; ln(N); ln(P9); γ_i | P5:P7b P7b:ln(N) ln(N):P10 P5:P10 P7b:P10 | 0.891 | 0.345g | 0.051g | 0.069g |
| MR_14 | ln(LS3) | $\lambda^{-1/2}$; ln(P3); P4; P5; P7b; ln(N); ln(P9); γ_i | P5:P7b | 0.865 | 0.338g | 0.057g | 0.077g |

853

854

855 Table 3. Characteristics of the regression models constructed for the definition of LS1 and LS2

| Model | Variables | | Interactions | R^2 | ε_{max} | MAE | RMSE |
|---------------|--------------|--|---------------|-------|---------------------|--------|--------|
| | Output | Input | | | | | |
| <i>MR_LS1</i> | $\ln(LS1+c)$ | $\lambda; s; \ln(P3); P4; P5; \ln(P6); P7b; \ln(N); \ln(P9)$ | <i>P5:P7b</i> | 0.811 | 0.319g | 0.057g | 0.079g |
| <i>MR_LS2</i> | $\ln(LS2)$ | <i>LS1; LS3</i> | - | 0.977 | 0.143g | 0.022g | 0.028g |

856

857

858 Table 4. Characteristics of the ANN regression models constructed for the definition of LS1 and LS3

| Model | Variables | | Interactions | R^2 | ϵ_{max} | MAE | RMSE |
|----------------|--------------|--|--------------|-------|------------------|--------|--------|
| | Output | Input | | | | | |
| <i>ANN_LS1</i> | $\ln(LS1+c)$ | $\lambda; s; \ln(P3); P4; P5; \ln(P6); P7b; \ln(N); \ln(P9)$ | - | 0.868 | 0.321g | 0.044g | 0.066g |
| <i>ANN_LS3</i> | $\ln(LS3)$ | $\lambda; s; P3; P4; P5; P6; P7a; P7b; N; P9; \gamma_i$ | - | 0.912 | 0.286g | 0.048g | 0.062g |

859

860

861 Table 5. Application of regression models to [Mendes and Lourenço 2015] and comparison of the results

| Model | P1 | P2 | P3 | P4 | P5 | P6 | P7a | P7b | P8 | P9 | P10 | LS3(g) | | |
|-------|------|-------|----|----|----|----|------|------|----|----|------|------------|--------|---------|
| | | | | | | | | | | | | Literature | MR_LS3 | ANN_LS3 |
| Y | 7.06 | 12.45 | 3 | 2 | 1 | 1 | 0 | 0.33 | 4 | 1 | 0.46 | 0.10 | 0.12 | 0.14 |
| X | 7.06 | 9.45 | 3 | 2 | 1 | 1 | 0.33 | 0 | 4 | 1 | 0.59 | 0.46 | 0.38 | 0.42 |
| Y(+) | 7.06 | 12.45 | 2 | 2 | 1 | 1 | 0 | 0.33 | 4 | 1 | 0.46 | 0.15 | 0.16 | 0.17 |
| X(+) | 7.06 | 9.45 | 2 | 2 | 1 | 1 | 0.33 | 0 | 4 | 1 | 0.59 | 0.51 | 0.48 | 0.56 |
| Y(-) | 7.06 | 12.45 | 4 | 2 | 1 | 1 | 0 | 0.33 | 4 | 1 | 0.46 | 0.07 | 0.10 | 0.12 |
| X(-) | 7.06 | 9.45 | 4 | 2 | 1 | 1 | 0.33 | 0 | 4 | 1 | 0.59 | 0.29 | 0.30 | 0.31 |

862

863

864 Table 6. Application of regression models to [Magenes et al. 2014] and comparison of the results

| Model | P1 | P2 | P3 | P4 | P5 | P6 | P7a | P7b | P8 | P9 | P10 | LS3(g) | | |
|----------|------|------|----|----|----|----|------|------|----|----|------|------------|--------|---------|
| | | | | | | | | | | | | Literature | MR_LS3 | ANN_LS3 |
| +Y (URM) | 8.35 | 5.2 | 2 | 2 | 4 | 2 | 0.1 | 0.07 | 2 | 1 | 0.46 | - | 0.38 | 0.32 |
| -Y (URM) | 8.35 | 5.2 | 2 | 2 | 4 | 2 | 0.32 | 0.07 | 2 | 1 | 0.46 | - | 0.40 | 0.35 |
| +X (URM) | 8.35 | 3.75 | 2 | 2 | 4 | 1 | 0 | 0.22 | 2 | 1 | 0.61 | 0.43 | 0.41 | 0.36 |
| -X (URM) | 8.35 | 3.75 | 2 | 2 | 4 | 1 | 0.14 | 0.22 | 2 | 1 | 0.61 | 0.43 | 0.43 | 0.38 |
| +Y (RM) | 8.35 | 5.2 | 2 | 2 | 2 | 1 | 0.1 | 0.07 | 2 | 2 | 0.46 | - | 0.58 | 0.60 |
| -Y (RM) | 8.35 | 5.2 | 2 | 2 | 2 | 1 | 0.32 | 0.07 | 2 | 2 | 0.46 | - | 0.62 | 0.66 |
| +X (RM) | 8.35 | 3.75 | 2 | 2 | 2 | 1 | 0 | 0.22 | 2 | 2 | 0.61 | 0.54 | 0.51 | 0.58 |
| -X (RM) | 8.35 | 3.75 | 2 | 2 | 2 | 1 | 0.14 | 0.22 | 2 | 2 | 0.61 | 0.54 | 0.53 | 0.62 |

865

866

867 Table 7. Application of regression models to [Kallioras et al. 2018] and comparison of the results

| Model | P1 | P2 | P3 | P4 | P5 | P6 | P7a | P7b | P8 | P9 | P10 | LS3(g) | | | LS1(g) | | |
|-------|----|------|----|----|----|----|------|------|----|----|------|-------------|--------|---------|-------------|--------|---------|
| | | | | | | | | | | | | Lit. | MR_LS3 | ANN_LS3 | Lit. | MR_LS1 | ANN_LS1 |
| +Y | 13 | 4.04 | 1 | 2 | 3 | 1 | 0.20 | 0.18 | 2 | 1 | 0.54 | 0.54 | 0.54 | 0.41 | 0.39 | 0.35 | 0.34 |
| -Y | 13 | 4.91 | 1 | 2 | 3 | 1 | 0.18 | 0.18 | 2 | 1 | 0.54 | 0.54 | 0.52 | 0.39 | 0.39 | 0.32 | 0.31 |

868

869

870 Table 8. Summary of the results obtained for the application of the regression models to all the cases studied

| | LS3(g) | | | | | | | | | | | | |
|-------------------|----------------------------|-------------|-----------------------|-------------|-------------------------|---------------------|-------------|-------------|-------------|------------------------|-------------|-------------------------|------------|
| | [Mendes and Lourenço 2015] | | [Magenes et al. 2014] | | [Kallioras et al. 2018] | [Betti et al. 2014] | | | | [Mouzakis et al. 2012] | | [Benedetti et al. 1998] | |
| | Y | X | URM | RM | Y | +X | -X | +Y | -Y | URM | RM | STM | BM |
| Literature | 0.10 | 0.46 | 0.43 | 0.54 | 0.54 | 0.27 | 0.29 | 0.29 | 0.29 | 0.48 | 0.88 | 0.19 | 0.3 |
| MR_LS3 | 0.12 | 0.38 | 0.43 | 0.53 | 0.54 | 0.23 | 0.23 | 0.27 | 0.28 | 0.52 | 1.01 | 0.20 | 0.29 |
| ANN_LS3 | 0.14 | 0.42 | 0.38 | 0.62 | 0.41 | 0.26 | 0.25 | 0.30 | 0.31 | 0.42 | 0.83 | 0.20 | 0.29 |

871

872

873 Table 9. SAVVAS formulation and procedure

| Step 1 | Definition of the seismic vulnerability assessment parameters | | | | | | | | | | |
|--------|---|---------|------------|------------|------------|------------|-------|-------|-----|------------|------------|
| | P1 | P2 | P3 | P4 | P5 | P6 | P7 | P8 | P9 | P10 | |
| | λ (h/t) | s (m) | $P3$ [1-4] | $P4$ [1-4] | $P5$ [1-4] | $P6$ [1-4] | $P7a$ | $P7b$ | N | $P9$ [1-4] | γ_i |
| Step 2 | Calculation of the load factors associated to the limit states in each main direction i | | | | | | | | | | |
| | $LS1_i(g) = e^{(1.97-0.06\lambda-0.1s-0.68\ln(P3)-0.14P4-0.28P5-0.39\ln(P6)-3.43P7b-0.82\ln(N)-2.27\ln(P9)+0.63P5P7b) - c}$ $LS2_i(g) = 0.16 \times LS1(g) + 0.78 \times LS3(g)$ $LS3_i(g) = e^{(2.16-0.04\lambda-0.05s-0.24P3-0.16P4-0.28P5-0.08P6+0.3P7a-2.79P7b-0.37N-0.15P9+0.74\gamma_i+0.44P5P7b)}$ | | | | | | | | | | |
| Step 3 | Calculation of the global load factors defining the limit states of the building | | | | | | | | | | |
| | $LS1(g) = \min(LS1_i(g))$ $LS2(g) = \min(LS2_i(g))$ $LS3(g) = \min(LS3_i(g))$ | | | | | | | | | | |

874